http://dx.doi.org/10.1016/j.jmst.2019.07.052

Deformation behavior and microstructure evolution of titanium alloys with lamellar microstructure in hot working process: A review

Abstract

Titanium alloys have gained extensive application in the fields of aircrafts, aerospace and medicine due to their excellent comprehensive properties. In order to obtain fine microstructure and favorable properties, a well-designed multi-step thermomechanical processing (TMP) are necessary in the manufacturing of titanium components. Especially, the subtransus processing intending to breakdown the lamellar microstructure after primary hot working is a very critical step, which plays key role in the final microstructure and performance tailoring. Thus, many researchers have made great efforts to investigate the mechanisms and laws of microstructure evolution and flow behavior in the subtransus processing of titanium alloy with lamellar microstructure. The recent relevant experimental and modelling achievements were reviewed in this paper. Firstly, the characteristics of the initial lamellar microstructure were first discussed. Then, the microstructure evolution during subtransus processing were summarized. Especially, the globularization of lamellar α is discussed in detail from three aspects, i.e., the globularization mechanism, heterogeneity and kinetics. The typical feature of flow behavior and various explanations for the significant flow softening were summarized. Besides, the advances in the modelling of microstructure evolution and flow behavior in the subtransus processing were also described. Finally, some puzzles and challenges needing more research efforts in the investigations of microstructure evolution and flow behavior of titanium alloy with lamellar microstructure were presented.

Key words: titanium alloy, lamellar microstructure, deformation behavior, microstructure evolution

1. Introduction

Titanium alloys have gained extensive applications in the fields of aircrafts, chemical processing, marine and medicine due to its excellent properties such as high specific strength, good thermal stability, low Young's modulus and excellent corrosion resistance [1-3]. Especially, the titanium alloy are widely used to manufacture the structural components and become an indispensable structural material in the aviation industry. The amount of titanium alloys used in advanced airplanes reaches 30%-50% weight of the total structure, for example, it reaches 41% in F-22 fighters [4,5]. These titanium alloy components often serve as key load bearing structures under severe conditions, which

puts very high requirements on its microstructure and mechanical properties.

In order to obtain fine microstructure and favorable mechanical properties, the thermomechanical processing (TMP) involving a series of steps, each step has specific microstructural goal, is usually employed to manufacture these components [6,7]. Generally, primary hot working and recrystallization annealing in the β-phase region is first conducted to eliminate the casting inhomogeneities, which produce a lamellar microstructure. However, the equiaxed microstructure presenting a better balance of strength and ductility is frequently desirable for final service. Therefore, the lamellar microstructure is commonly broken down (referred to as globularization) to get the desired equiaxed microstructure by subtransus processing. This process plays a very critical role in the microstructure tailoring for final service performance of titanium alloy components [8-10]. However, the microstructure evolution and deformation behavior are very complex and strongly dependent on the initial microstructure and processing conditions during the subtransus processing. Thus, this technological step represents the most important and difficult step during the TMP of titanium alloy from the workability and microstructure control standpoint.

Due to its great technological importance, extensive experimental and modelling investigations have been conducted on the microstructure evolution and deformation behavior during subtransus processing of lamellar microstructure. The research frontiers of this field mainly include the following four aspects:

(1) *Characteristics of the initial lamellar microstructure.* It mainly refers to the characteristics of morphology, distribution, parameters (the volume fraction, colony size and lamellar α thickness), crystallographic orientation and texture of the initial lamellar microstructure. These characteristics play significant role in the deformation mechanism and microstructure evolution. Thus, the development of lamellar microstructure and its dependences on the β processing parameters have been concerned.

(2) *Microstructure evolution during subtransus processing.* Globularization of lamellar α is the most significant microstructure evolution phenomenon as well as the goal of microstructure tailoring in the subtransus processing [7,8]. The globularization mechanism and break up process of lamellar α has always been the basic research on frontier. Meanwhile, the globularization kinetics and its dependence on the initial microstructure parameters (including the morphology, colony size, initial lamellar α thickness, etc.) and subtransus processing parameters (including the loading path, deformation temperature, strain rate, etc.) have also been investigated extensively. In addition, the heterogeneity of

globularization and the microtexture of obtained globular microstructure have also attracted some interest recently. On the other hand, the changes of geometrical and crystallographic orientations of lamellar α, kinking of lamellar α and shear band are also three main features of microstructure evolution needing concerns.

(3) *Flow behavior during subtransus processing.* Significant flow softening is the most important feature of flow behavior for hot working of lamellar microstructure [10]. Many researchers have been trying to reveal the underlying mechanisms of flow softening from the standpoints of deformation heating, dislocation substructure, dynamic globularization of lamellar α, kinking of lamellar α, loss of Hall-Petch strengthening, texture change, etc.

(4) *Modelling of the microstructure evolution and flow behavior.* Establishing the accurate prediction models of globularization kinetics and flow behavior of during hot deformation of lamellar microstructure to guide the TMP is the relentless pursuit for researchers. At present, the globularization and flow behavior are mainly modelled respectively by the empirical regression and statistical methods. Recently, the physically-based model, such as the internal state variable method, has been developed to realize the unified predictions of globularization kinetics and constitutive behavior of lamellar microstructure. It considers the underlying coupling mechanisms among microstructure development, plastic flow and processing conditions and has become a research hotspot.

This paper presents a critical review on the experimental results and modelling for hot deformation behavior and microstructure evolution of titanium alloy with lamellar microstructure, which were reported in international publications in recent years. The progresses can instruct the hot working of titanium alloy. Moreover, some puzzles and challenges needing more research efforts in this field are also summarized.

2. Characteristics of lamellar microstructure

During the TMP of titanium alloy, the lamellar microstructure produced after primary hot working in β-phase region play critical role in the subsequent deformation mechanism and microstructure evolution in subtransus processing. Thus, the development mechanism, morphology, size and crystallographic orientation of the lamellar microstructure have attracted lots of researches.

2.1 Development of lamellar microstructure

Fig.1 shows the typical lamellar microstructure after primary hot working in β-phase region. It consists of three micro-constituents: grain boundary α around the prior-β grain (α_{GB}),

lamellar/basket-weave α colonies (α_{WGB}) in the prior-β grain, and thin β layers separating the α lamellae. It is widely concluded that the development of lamellar microstructure is governed by the β→α phase transformation during cooling process from β-phase region to α/β phase region and goes through four stages (Fig.2 (a)) [11,12]: (1) α_{GB} allotriomorphs nucleate on β grain boundaries until complete coverage; (2) α_{GB} grow on one side of boundary; (3) α_{WGB} appear on the growing α_{GB} front; (4) α_{WGB} grow inside the initial β grains and forms the colonies. In addition, the β→α phase transformation is normally governed by the Burgers orientation relationship (BOR), which is described by {0001}α//{110} β and <11-20> α//<111>β (Fig.2(b)) [13,14]. Fig.3 gives the typical experimental crystallographic orientation map of lamellar microstructure and the local crystallographic orientation between the adjacent lamellar α and β phases (in the red ellipse of Fig.3(a)), respectively [15]. It can be found from Fig.3(b) that the (0001) plane and one of <11–20> directions of lamellar α phase are parallel to one of the {110} planes and one of the <111> directions of β phase, respectively, for the colony A, B and C. Theses mean that the adjacent lamellar α and β phases keep the BOR. The BOR may provide easy gliding transmission across α/β phase boundaries such that an individual α colony behaves as a single grain [9,16-18]. However, this orientation relationship may be broken during the subtransus processing, which will be discussed in Section 3.

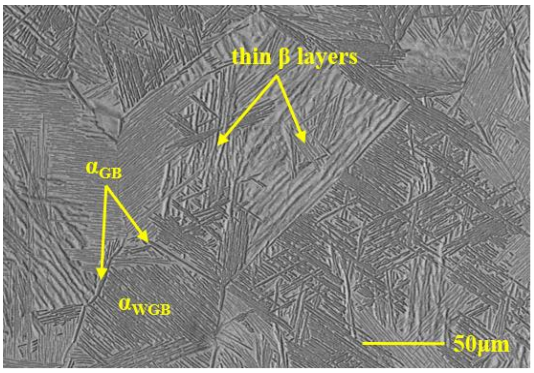

Fig.1. The typical lamellar microstructure after primary hot working in β-phase region (The microstructure of TA15 alloy after heating to 1020℃, hold 5 min then air cooled).

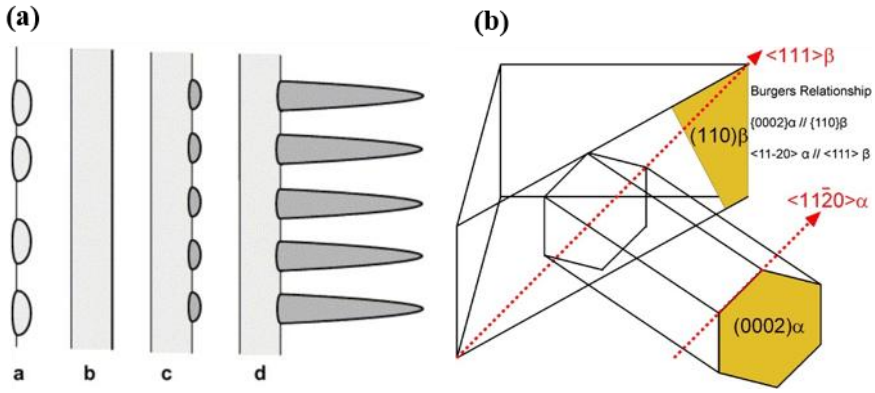

Fig.2. Schematic of formation process (a) [12] and Burgers relationship between α and β phase (b) [14] of lamellar microstructure.

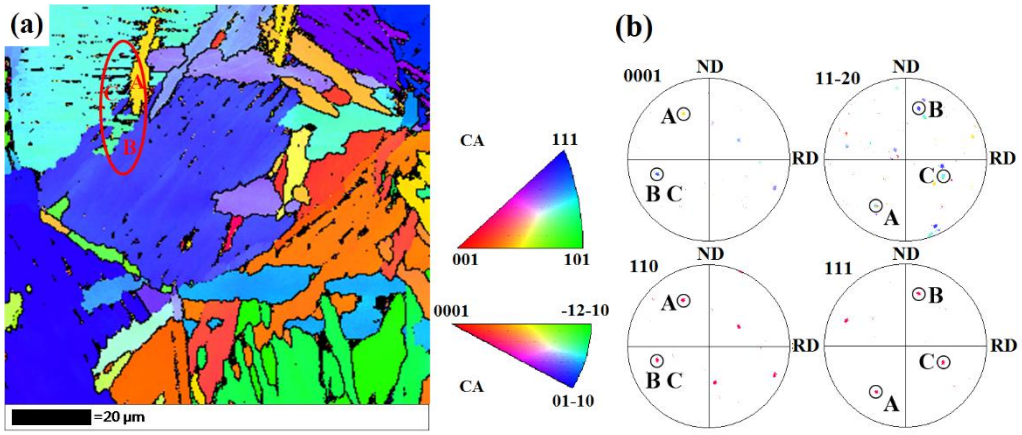

Fig.3. Typical orientation map (a) and orientation relationship between α and β phase (b) of lamellar microstructure [15].

As well known, α phase presents limited slip systems and the critical resolved shear stresses (CRSSs) of different slip systems are highly anisotropic. Its crystallographic orientation greatly affects the deformation behavior and microstructure evolution during deformation of lamellar microstructure. Based on the BOR as well as the symmetries of α phase (HCP structure) and β phase (BCC structure), twelve distinct α orientations (variants) can form in a single parent β grain. And they can produce six distinct types of misorientations between α variants, as summarized in Table 1 [19-22]. When all twelve α variants occur with equal probability, the β→α phase transformation is said to evolve without variant selection and the final α texture should be weaker than the initial one after α→β→α heat cycle. However, many experiments demonstrated that only a subset of the twelve α variants present and some α variants are more frequently observed than others, i.e. variant selection occurs [23,24]. The degree of variant selection (*DVS*) can be measured by

$$DVS=\sum_{i=1}^{6}|P_{ob}(i)-P_{random}(i)| \quad (1)$$

where $P_{ob}(i)$ is the probabilities of misorientation angle i from the observed results, and $P_{random}(i)$ is the corresponding probabilities in random condition shown in Table 1. If no variant selection occurs, *DVS*=0; if a single variant of α phase is able to percolate through the whole β grain, a maximum *DVS* (1.833) is reached [19].

Table 1 Misorientations between α variants (expressed in axis/angle pairs) inherited from the same parent β grain and the corresponding probabilities without variant selection [19].

Misorientation types	Rotation axis/angle	P_{random} (%)
A	I (identity)	8.3
B	[1 1 $\bar{2}$ 0]/60°	16.6
C	[10 $\bar{7}$ 17 3]/60.83°	33.3
D	[10 5 5 3]/63.26°	16.6
E	[7 17 10 0]/90°	16.6
F	[0 0 0 1]/10.53°	8.3

The above variant selection is mainly interpreted by the following four aspects: (1) the elastic strain energy generated by the β→α transformation. Humbert et al. [25,26] have proposed that the variants with minimum elastic strain energy are preferentially nucleated. (2) the selective formation of grain boundary α phase. It has been reported that the variant selection will occur in the formation of grain boundary α phase when the neighboring prior β grains share one common (110) β pole or have close orientation, i.e., the α variants with (0001) pole parallel with the common (110) β pole are selected [13,16,27]. (3) the pre-existing defects within β phase. Gey et al. [28] found that higher defect density related to (110)[111] slip system could act as nucleation and growth sites of selective variants. Qiu et al. [19] further proposed that the elastic interaction between α precipitates and dislocations governs the variant selection during nucleation stage, while the habit plane orientations of α precipitates relative to the dislocation lines dominates the variant selection during growth stage. Besides, the edge type dislocation has a much stronger effect than that of the screw type on the variant selection. (4) the autocatalysis effect caused by the relaxation of local stress related to pre-existing α lath. It has been found that there exists largely nonuniform stress field around a pre-existing α lamellae, which will produce different interactions with various α variants [23]. Both of the experimental and

simulation results suggest that the orientation relationship between new-formed α variant and pre-existing α most belong to the following three types, i.e., $[11\bar{2}0]_{\alpha}$/60°-type, $[\bar{1}0553]_{\alpha}$/63.26°-type and $[0001]_{\alpha}$/10.53°-type, which will lead to variant selection to some extent.

2.2 Dependence of lamellar microstructure on β processing

The β processing parameters as well as the influencing mechanisms and resulting microstructure characteristics are summarized in a tabulated form in Fig.4. Increasing the β processing temperature and holding time can gratefully promote the β grain growth, then improve the α colony size and α variant selection at β grain boundaries having a common (110) pole. The deformation parameters (deformation mode, strain and strain rate) mainly influence the grain refining, texture and bring pre-dislocation in prior-β microstructure. This will then affect the β grain size, α morphology, α colony size and α variant selection. Specifically, the defamation parameters strongly affect the β grain size due to the variation of dynamic recrystallization behavior. Seshacharyulu and Dutta [29] found that because the β → α transformation mechanism changes from homogeneous precipitation to heterogeneous precipitation, the α morphology changes from lamella to equiaxed grain when the stain rate increased from low value ($\leqslant 0.1 s^{-1}$) to high value ($1\sim100\ s^{-1}$). Zhao et al. [24] found that strong β texture in (110) pole figure means a large chance of neighboring β grains with nearly parallel (110) pole, which will promote variant selection and coarser α colonies. Besides, the role of pre-dislocation produced by deformation in the α variant selection has been investigated by Qiu et al. [19], as demonstrated above. Cooling rate is the most critical parameter determining the nucleation mechanism, location and kinetic of β → α phase transformation, which play great and comprehensive role in the characteristics of lamellar microstructure including the α morphology, α colony size, lamellar α thickness and α variant selection. Fig.5 schematically summarizes the general effect of cooling rate on the microstructure characteristics. At lower cooling rate, α platelets only nucleate at grain boundary and then grow inside, while some α platelets nucleate homogeneously inside the grain at higher cooling rate [12,30]. The content of α_{GB}, α colony size and lamellar α thickness all decrease with the increase of cooling rate [8,10,30-33]. Moreover, the variant selection at sample with (110) β texture also decreases with increasing cooling rates [24,34].

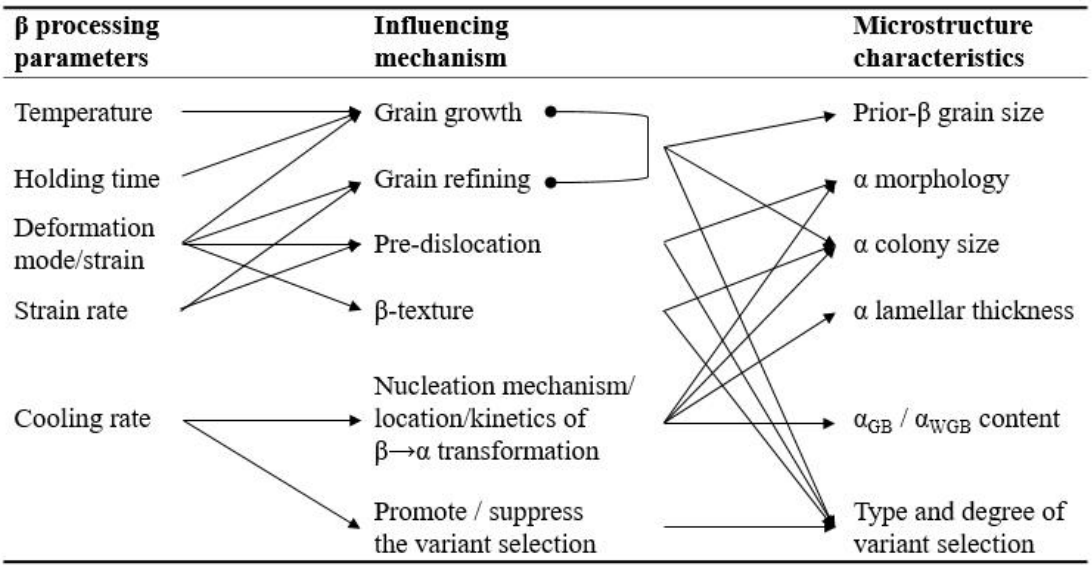

Fig.4. Important parameters of β processing, influencing mechanisms and resulting microstructure features of lamellar microstructure.

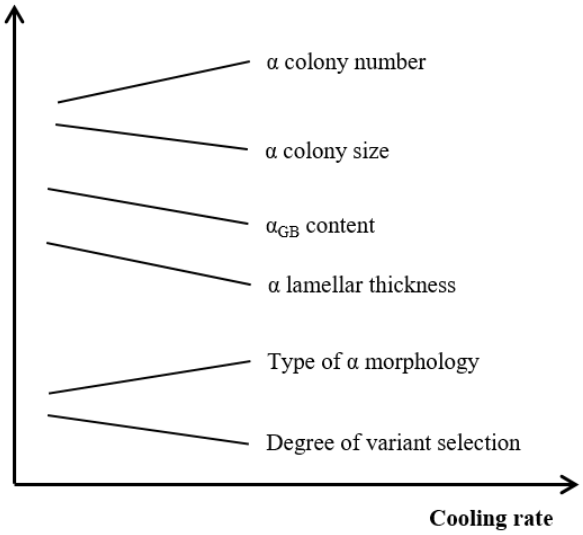

Fig.5. General influence law of cooling rate on the microstructure features of lamellar microstructure.

3. Microstructure evolution during subtransus processing of lamellar microstructure

3.1 Mechanical and crystallographic texture change of lamellar α

The rotation of lamellar α is one of the important microstructure change phenomenon during hot deformation of lamellar microstructure. Fig.6 shows the typical evolution of lamellar α during compression of Ti-6Al-4V alloy [9]. Generally, the evolution of lamellar α is associated with their geometrical orientations relative to the compression axis. If the trace of lamellar α was parallel to the compression direction, it tended to be kinked (circled areas in Fig.6(b) and (c)). Otherwise, the lamellar α would rotate with strain toward ‘‘softer’’ orientations and progressively realign their traces

perpendicular to compression direction. Fig.7 shows the quantitative measurement results on the rotation of lamellar α [10]. It was evaluated through the frequency distribution of lamellar α orientations as a function of strain, in which the lamellar α orientation means the angle between the trace of a given lamellae and the compression axis (denoted as θ). It can be seen that the orientation distribution substantially changes at relatively low strains (of the order of 0.50) and became sharper around θ=90° at larger strains (greater than 1.0).

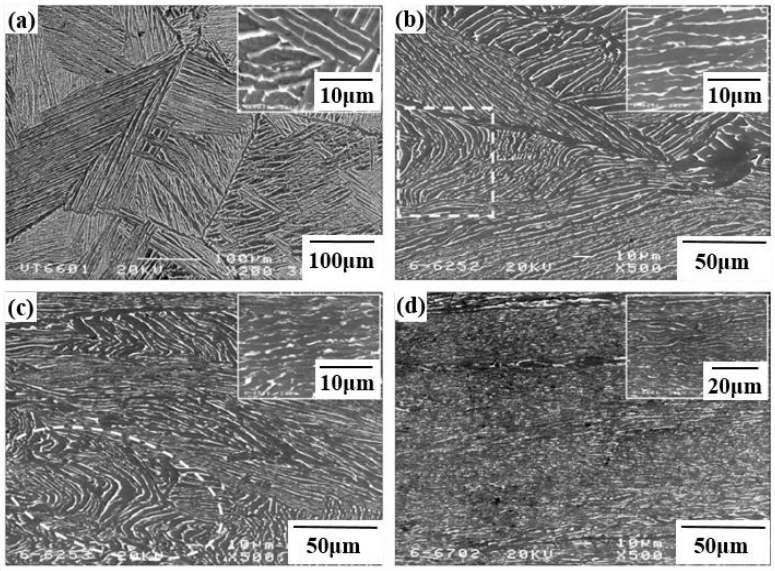

Fig.6 The typical evolution of lamellar α during hot deformation of Ti-6Al-4V alloy with lamellar microstructure at 600℃ and 0.001s^{-1}: (a) prior to deformation, and after height reductions of (b) 25%, (c) 50% and (d) 70% [9].

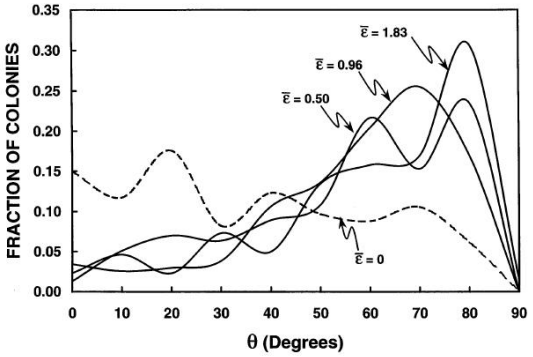

Fig.7. Orientation distribution of lamellar α traces relative to the compression axis for Ti-6Al-4V with lamellar microstructure deformed at 900℃, 0.1s^{-1} to different strains [10].

The rotation of lamellar α was necessarily accompanied by the change of crystallographic orientation feature of microstructure. To differentiate two types of orientation, the preferred geometrical orientation of morphology feature (lamellar α trace) and crystallographic orientation are

called as mechanical texture and crystallographic texture, respectively [35]. Perumal et al. [36] presented the typical crystallographic texture evolution of lamellar α during hot deformation, as shown in Fig.8. The crystallographic texture evolution will change the dislocation slip behavior and average Taylor factor, then affect the flow behavior, which will be described in Section 4.2. On the other hand, the BOR between lamellar α and β phase in initial lamellar microstructure will be broken, meanwhile the initial semi-coherent α/β interface will change to non-coherent interface with the variation of mechanical texture. This is because the adjacent α and β lamellae may rotate relative to each other, which produces the localized flow at α/β boundary and the breakdown of BOR. Besides, a significant orientation spread within each α colony as well as within individual α lamellae will be formed due to the activation of different slip systems [9,37]. These changes of crystallographic orientation features play great effects on the globularization behavior of lamellar microstructure.

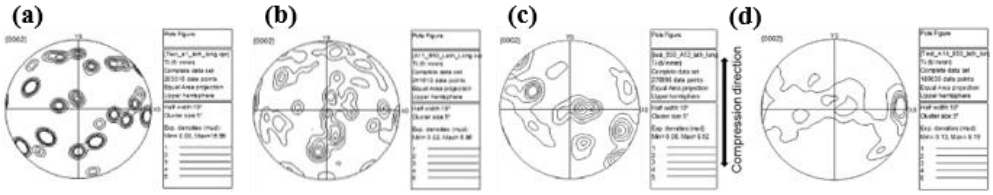

Fig.8. The typical crystallographic texture evolution of lamellar α during hot deformation of Ti-6Al-4V alloy with lamellar microstructure at 950℃ and $0.1s^{-1}$: (a) ε= 0, (b) ε= 0.2, (c) ε = 0.7 and (d) ε = 1.0 [36].

3.2 Kinking of lamellar α

Fig.9 shows the typical kinking of lamellar α, which is also an important phenomenon during the hot deformation of lamellar microstructure [9,10,15,32,38-41]. It is found that the frequency and degree of kinking vary from one colony to another strongly depending on their orientation with respect to the compression axis. It preferentially takes place at the colony with lamellar trace nearly parallel to the compression axis. And, experimental results show that substantial platelet kinking usually occur at lower strains (ε<0.3).

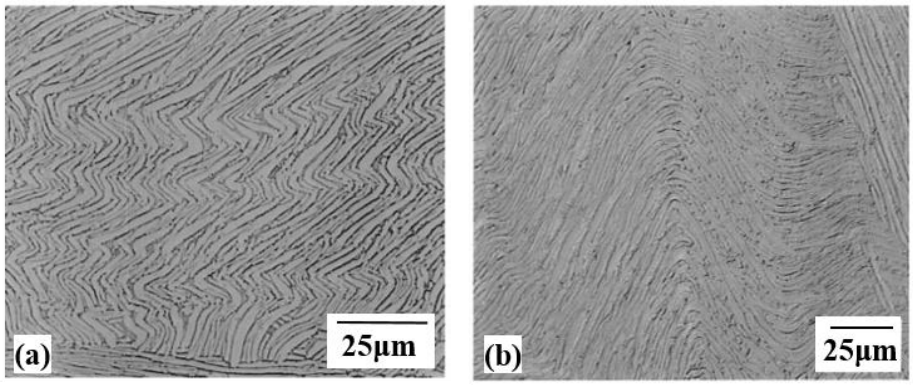

Fig.9. The kinking of lamellar colonies during hot compression (a) and tension (b) of Ti-6Al-4V at 900°C, $0.1s^{-1}$. The compression/tension axis is vertical in both micrographs. [40]

At present, there are two different explanations for the formation mechanism of kinking of lamellar α. Some researchers think it is closely related to the development of shear bands within α colonies [9,38]. However, other researchers think it may be a form of plastic buckling analogous to that occurs during the compression of slender beams [10,15,32]. Fig.10 shows the SEM image and corresponding inverse pole figure of a region containing the kinking of lamellar α colonies (colony A, B, C, D) from the authors' work [15]. It is found that the lamellar α and β phases within colony still nearly obey the BOR after great bending, which suggests that the kinking occurs in the manner of "rigid rotation". Moreover, colonies C and D are very close in location but bended in the opposite directions, which is also applicable for the colonies A and B. These suggest that the kinking of lamellar α is closely related to the plastic buckling rather than the shear band. It should be noted that the significant crystallographic rotation, low-angle boundaries (LABs) and high-angle boundaries (HABs) will be produced after the kinking of lamellar α, as shown in Fig.10(b). The resulted HABs will contribute to the "fragmentation" of initial lamellar, and is helpful to promote the globularization of lamellar microstructure.

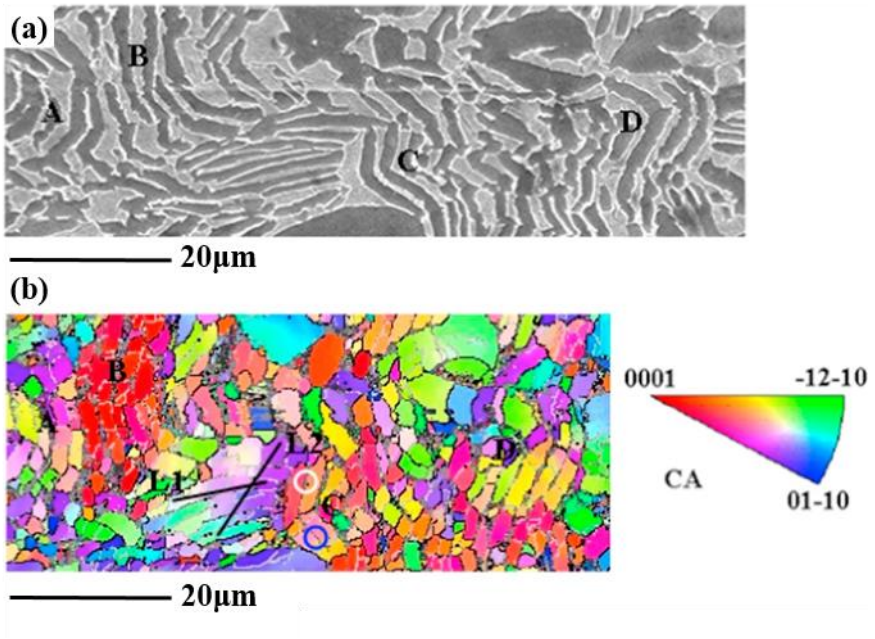

Fig.10. The SEM image (a) and corresponding inverse pole figure (b) of a region containing kinking of lamellar α in the hot deformation of TA15 alloy with lamellar microstructure [15]. (In the inverse pole figure, β phase is indicated by gray areas, the black lines correspond to HABs, and the silver lines represent LABs)

3.3 Globularization of lamellar α

Dynamic globularization of lamellar α is the most important microstructure evolution behavior during hot deformation of titanium alloys with lamellar microstructure. Lots of investigations have been conducted on the dynamic globularization behavior of lamellar α [9,10,32,41-62], which will be reviewed from three aspects, i.e., the mechanism, heterogeneity and kinetic of globularization, in this section.

(1) Globularization mechanism

Many studies indicate that the globularization of lamellar α includes three stages, i.e., the formation of high-energy defects, the instability of lamellar α induced by the high-energy defects, and the coarsening of split α grains, as shown in Fig.11 [43-45]. The first stage introduces the high-energy defects by the recovery, recrystallization, localized shearing, twinning or kinking during deformation. The high-energy defects mainly refer to the structural defects like dislocations, twins and morphological features like kinks, striations, etc., which manifests the formation of intra-α substructure and the loss of α/β interfacial coherency [37,38,46-51]. They provide the required driving force for the subsequent instability of lamellar α, which will split the lamellae to short ones or spheroids through

mass transport. For now, various instability types have been observed, consisting of the direct cylinderization via the recession of edge termination, boundary splitting via thermal grooving, edge spheroidization via the ovulation of ridges. Furthermore, the occurrence conditions of these types of instabilities have also been demonstrated, which mainly depend on the aspect ratio of lamellae, the interfacial energy ratio between intra-α and α/β boundaries, the dominating mechanism of mass transfer (volume or interfacial diffusion), etc. [49,52,53]. Then, the split α will further get spheroidization and coarsening by the termination migration and Ostwald ripening. Both of them are driven by the reduction of interfacial energy. The termination migration refers to the mass transfer from the curved termination to the adjacent flat surface in the same lamellae or any neighboring lamellae under the chemical potential gradient induced by the curvature difference. The Ostwald ripening occurs through the growth of large grains and the expense of small grains [43,44,54].

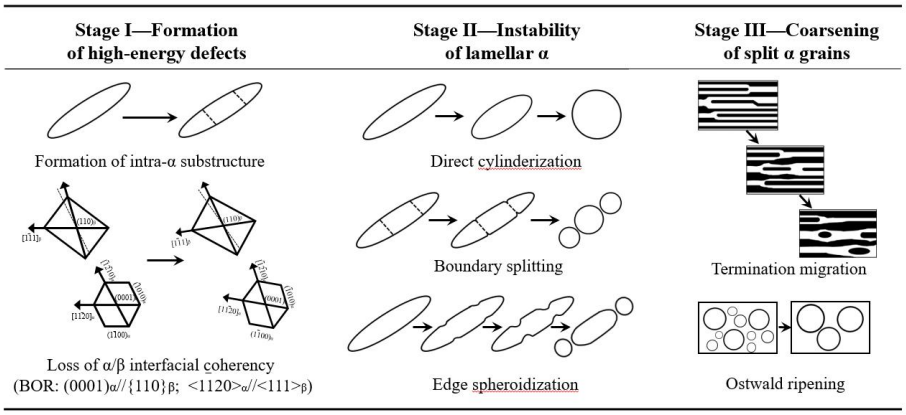

Fig.11. The schematic of globularization mechanism of lamellar α.

(2) Globularization heterogeneity

Globularization heterogeneity is a common but undesirable phenomenon for the globularization of lamellar microstructure because it leads to the property heterogeneity. Traditionally, globularization heterogeneity refers to the inhomogeneous globularization fraction distribution at microstructure scale, as shown in Fig.12 [45]. It is mainly caused by the heterogeneous deformation relating to the geometrical and crystallographic orientation feature of lamellar microstructure. It is well known that both of the geometrical and crystallographic orientations of α colony are different to each other in lamellar microstructure. As described in Section 3.1, different α colonies will present different dislocation slip behavior and α/β interface property evolution dependent on their geometrical and crystallographic orientations related to the loading direction. This will result in various globularization efficiency for different colonies and then the globularization heterogeneity. Mironov et al. [9] found the

lamellar α parallel to loading direction is easier to break up presenting higher globularization efficiency in the warm working of Ti-6Al-4V alloy. Bieler et al. [39] and Roy et al. [49] analyzed the effects crystallographic orientation on the deformation behavior and globularization efficiency of lamellar α by experiment. They found that the "soft" oriented lamellar α deforms by multiple slip (basal <a> plus prism <a> slips; or prism <a> plus pyramidal <c+a> slips) and presents high globularization efficiency. Moreover, a semi-quantitative representation of globularization efficiency as a function of c-axis tilt from compression direction (Taylor factor) of lamellar α was established by Bieler et al. [39], as shown in Fig.13. In addition, the heterogeneous loss of α/β interface coherency is also another important factor leading to the globularization heterogeneity of lamellar α [37]. However, there is still a lack of deep understand on this effect mechanism at present.

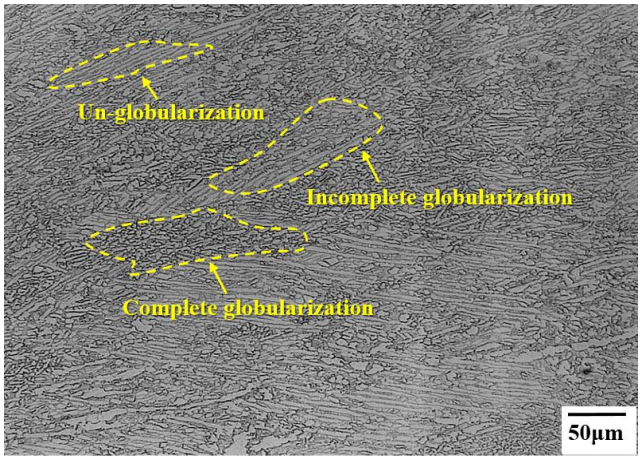

Fig.12. The globularization heterogeneity after hot deformation of ELI grade Ti-6Al-4V alloy with lamellar microstructure [45].

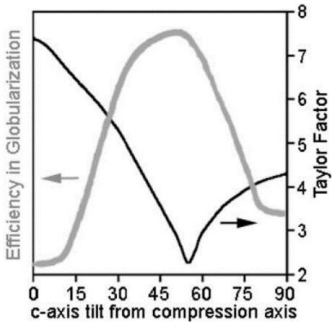

Fig.13. The semi-quantitative relationship between globularization efficiency and c-axis tilt from compression direction (Taylor factor) of lamellar α [39].

Recent studies [55,56] suggested that the globularization heterogeneity will also produce texture heterogeneity in the subtransus processing of lamellar microstructure. Its feature is the formation of different macro-zones showing various microtexture after globularization process, as shown in Fig.14.

The macro-zone corresponds to a region where a majority of globularized α grains present close crystallographic orientation, whose formation is related to the colony structure of lamellar microstructure and deformation characteristics of HCP α phase. The lamellae α in a same colony exhibit the same geometrical and crystallographic orientation and close stress state, thus, present similar deformation feature and globularization behavior. It produces a cluster of globularized α grains with close crystallographic orientation, i.e., macro-zone. Furthermore, the deformation of HCP α develops a sharp deformation texture with a limited number of texture components, which causes that the globularized α grains inherited from the current and neighboring globularization clusters may rotate toward the same texture component. This procedure will extend the macro-zone to a larger size than the prior colony [55].

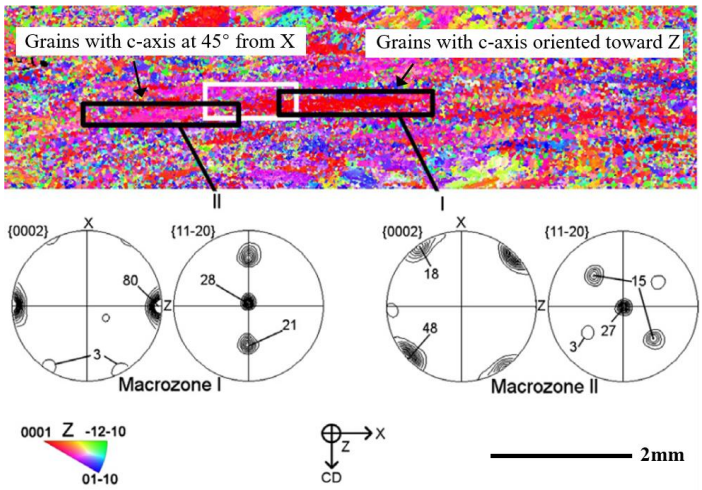

Fig.14. The texture heterogeneity after subtransus processing of TIMETAL 834 alloy with lamellar microstructure [55].

As for the suppression of globularization heterogeneity, limited investigations have been conducted. Semiatin et al. [38] indicated that increasing the deformation temperature and amount can improve the deformation homogeneity and globularization efficiency, then weaken the globularization heterogeneity. However, more comprehensive works should be conducted on the underlying mechanisms and control method for the globularization heterogeneity and resulted texture heterogeneity.

(3) Globularization kinetics

Dynamic globularization kinetics have been experimentally revealed to usually present the sigmoidal tendency for the variation of globularization fraction with strain [57,58]. The critical strain for initiation of globularization and globularization rate are two key factors to assess the

globularization kinetics. They are found to be mainly dependent on the deformation conditions and initial lamellar microstructure features. Wang et al. [57] found that the critical strain for initiation of globularization increases with the increase of deformation temperature and decrease of strain rate. Semiatin et al. [10] suggested that at lower strain rate ($0.0001s^{-1}$), where the deformation-heating can be negligible, the deformation temperature plays little effect on the globularization rate. However, at higher strain rate (0.1 and $10s^{-1}$), the dependence of globularization rate on deformation temperature is confused due to the temperature rises caused by deformation-heating. In addition, it was also pointed out that the dependence on temperature and strain rate of globularization rate is of second-order importance compared to the effects of deformation amount. As far as the effects of initial lamellar microstructure be considered, it is found that the dynamic globularization kinetic increases with the α colony size for microstructures [59]. The fine acicular lamellar α exhibits faster globularization than the coarse lamellar α due to the easier boundary splitting for thin lamellar α [32]. And the colony structure inserted by short and consistently oriented lamellar α presents slower globularization rate than the long and random oriented lamellae, because the latter one usually kinks first before break-up resulting in the delay of dynamic globularization [60].

The above investigations all focus on the one-stage uniaxial hot deformation of lamellar microstructure. It has also been found that the change of strain path significantly influences the dynamic globularization kinetic of lamellar α. Fan et al. [60] demonstrated that two-stage compression with vertical directions yields a higher dynamic globularization rate compared to that with parallel directions, as shown in Fig.15. While, the two-stage compression with strain path reversal leads to a reduction in the dynamic globularization kinetics compared with monotonic deformation [61]. On the other hand, Fan and his workers [62] also found that the interrupted multiple-pass compression with inter-pass holding pronouncedly affects the globularization kinetics. Fig.16 shows the schematic of globularization process during interrupted compression. Different from the one-stage deformation, the static recovery in α phase and static recrystallization in β phase occur during the inter-pass holding for interrupted compression. These result in the formation of α/α substructure and loss of α/β interface coherency, thus, accelerate the boundary sliding, strain partitioning and globularization efficiency in the subsequent compression. Besides, they have found that the final globularized fraction increases in a sigmoidal way with the holding time, interrupted strain and deformation pass.

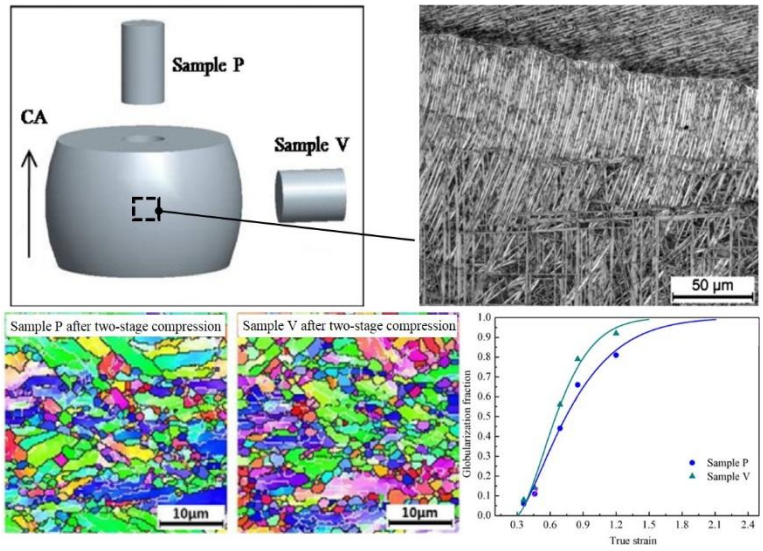

Fig.15. Schematic representation of two-stage compression with parallel (Sample P) or vertical (Sample V) directions in the second compression stage and the corresponding results of globularization kinetics [60].

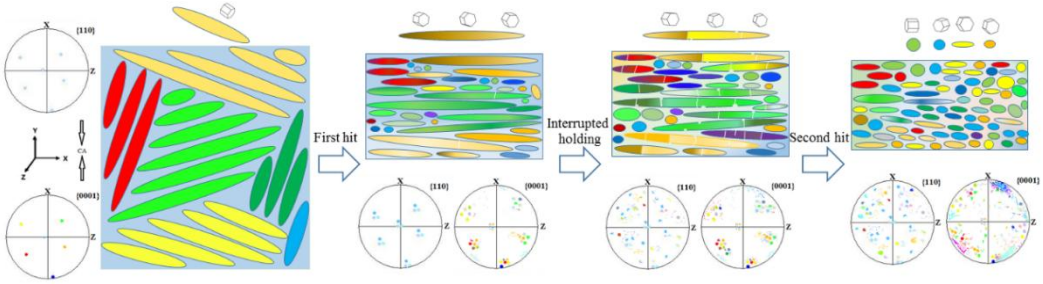

Fig.16. Schematic representation of globularization process of lamellar α during the interrupted compression [62].

3.4 Adiabatic shear band and flow localization

Adiabatic shear band and flow localization are also common phenomena in the hot working of lamellar microstructure, as shown in Fig.17 [63,64,65]. Their occurrences are related to the local temperature rise caused by deformation heating. The temperature rise would increase the dislocation mobility, reduce the deformation resistance and then lead to larger deformation in the central part of compressed sample. This will lead to the shear band and flow localization. Quantities of investigations suggest that the adiabatic shear band and flow localization are more likely to produce at relatively low temperature and high strain rate. And, their area is mainly related to the stress state and crystallographic orientation distribution of initial microstructure, which usually cross several or dozens of initial β grains [38,63-68]. The local large deformation caused by shear band and flow localization will greatly promote the globularization of lamellar α, thus lead to significant inhomogeneous microstructure

[69,70]. Moreover, the severe shear band and flow localization may cause micro-crack. Therefore, the shear band and flow localization should be avoided in the design of TMP for lamellar microstructure.

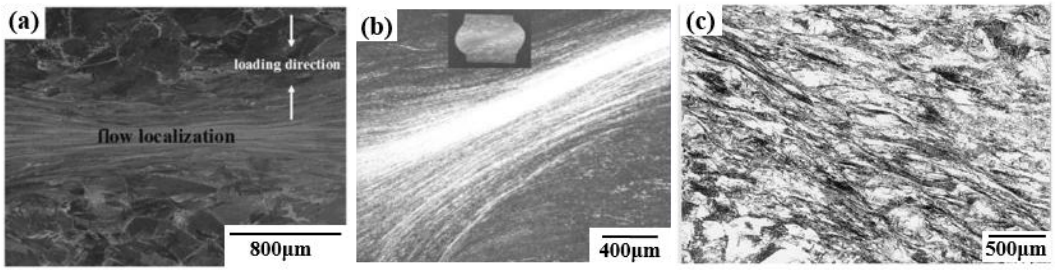

Fig.17. Shear band and flow localization in the hot working of titanium alloy with lamellar microstructure: (a) Ti17 alloy deformed at 780℃, $10s^{-1}$ and 30% [63]; (b) Ti-5Al-2Sn-2Zr-4Mo-4Cr alloy deformed at 770℃, $5s^{-1}$ and 60% [64]; (c) Ti-6Al-4V alloy deformed at 850℃, $10s^{-1}$ and 50% [65].

4. Flow behavior during subtransus processing of lamellar microstructure

4.1 Typical flow softening behavior and rules

Fig.18 shows the typical flow behavior during subtransus processing of lamellar microstructure, which exhibits a significant flow softening compared to that of equiaxed microstructure. During deformation, its stress quickly reaches the peak stress at a low strain with the order of 0.04 and then decreases with further straining exhibiting significant flow softening. When the strain increases to the order of 0.7, the flow stress reaches a steady state. The flow softening degree (γ) can be evaluated by the ratio of the difference between peak stress and steady stress to the peak stress:

$$\gamma = (\sigma_p - \sigma_{ss})/\sigma_p \tag{2}$$

where σ_p is the peak stress and σ_{ss} is the steady stress. The flow softening degree strongly depends on the deformation parameters and initial microstructure, whose underlying mechanisms and detail rules will be reviewed below.

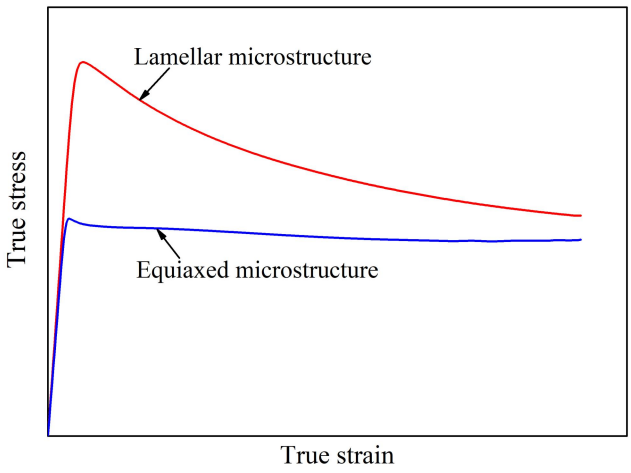

Fig.18. Typical flow curve of titanium alloy with lamellar microstructure and equiaxed microstructure during subtransus processing.

4.2 Flow softening mechanisms and rules

The flow softening may be relative to many physical processes, such as the deformation heating, dislocation substructure, dynamic globularization of lamellar α, kinking of lamellar α, loss of Hall-Petch strengthening, shear band formation, texture change, etc. The main investigation results on this subject are summarized according to the causes as follows.

（1）Deformation heating

The deformation heating can be individually classified into a group, which is different to other softening sources related to the microstructure changes. When titanium alloys deform at an elevated temperature, the deformation-induced heat can not be conducted and dissipated into the die in a short time due to its low thermal conductivity. This will lead to the temperature rise (ΔT), which promotes the mobility of dislocation and then reduces the flow stress, i.e., flow softening. Thus, the measured flow curves are usually corrected to separate the softening effect of deformation heating from those related to microstructure changes. The correcting approach can be found in [71,72] as follow. The ΔT during deformation can be calculated by

$$\Delta T = \frac{\eta\beta \int \sigma d\varepsilon}{\rho c} \tag{3}$$

where, β is the ratio of plastic deformation work converted into heat, which is usually taken as 0.95. σ is the flow stress, ε is the strain, ρ is the density, c is the specific heat, η is the adiabatic correction factor as follows:

$$\eta = \begin{cases} 1, \dot{\varepsilon} \geq 1s^{-1} \\ \frac{1}{3}(3 + log\dot{\varepsilon}), 10^{-3}s^{-1} < \dot{\varepsilon} < 1s^{-1} \\ 0, \dot{\varepsilon} \leq 10^{-3}s^{-1} \end{cases} \quad (4)$$

Then, the relationship among the flow stress, strain rate, strain and instantaneous temperature would be constructed. According to this relationship, the temperature-corrected flow curves at various nominal test temperatures (isothermal condition) could be determined. Semiatin et al. [10] quantitatively compared the softening extents related to deformation heating and microstructure changes at different conditions, as shown in Table 2. It is suggested that the temperature rise and flow softening caused by deformation heating are significant at higher strain rates and lower temperatures. However, it should be noted that the deformation heating contributes little to the total flow softening, while the microstructure related softening prevails at lower strain rates (<0.1s^{-1}).

Table 2 Comparisons between the softening extents related to deformation heating and microstructure changes at different conditions for a Ti-6Al-4V alloy with lamellar microstructure [10].

Temperature (°C)	Strain rate (s^{-1})	$\Delta\sigma/\sigma_p$ at $\bar{\varepsilon}$=0.50		
		Heating related softening	Microstructure related softening	Total softening
815	10^{-3}	0.00	0.26	0.26
815	10^{-1}	0.09	0.29	0.38
815	10^{1}	0.16	0.12	0.28
900	10^{-3}	0.00	0.23	0.23
900	10^{-1}	0.09	0.31	0.40
900	10^{1}	0.15	0.13	0.28
955	10^{-3}	0.00	0.16	0.16
955	10^{-1}	0.10	0.23	0.33
955	10^{1}	0.17	0.05	0.22

（2）Evolution of dislocation substructure and dynamic recovery (DRV)

It has been reported that the strain rate sensitivity of flow stress (m) locates in the range of 0.1~0.27 for hot deformation of lamellar microstructure [10]. This indicates that the dislocation glide and climb processes controls the deformation behavior. The DRV would occur and produces dislocation walls/pile-ups and subgrain structure within the lamellar α and β phases, as shown in Fig.19 [9,73,74]. It will decrease the dislocation density to some extent. Consequently, the evolution of dislocation substructure and DRV contribute to the flow softening. However, the experimental results of Semiatin et al. [10] suggested that this contribution is very small. They conducted interrupted compression-test and stopped deformation at the strain of 0.3. Then, the sample was held for 30 min to

produce sufficient recovery. After that, the sample was reloaded for an additional strain increment of 0.2. The reloading flow curve nearly continues at the end of interrupted flow curve, and is close to the flow curve without interruption. Thus, they concluded that the evolution of dislocation substructure and DRV weaken the working hardening to some extent in the early stages of deformation, however, contribute little to the significant softening in the later stage of deformation.

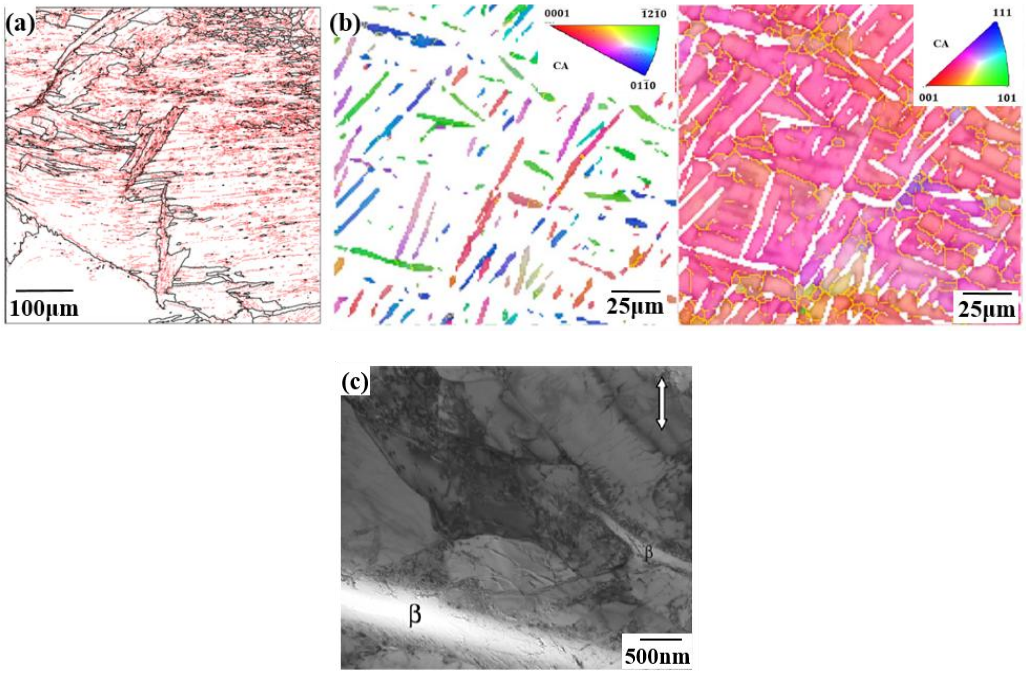

Fig.19. The dislocation substructure and subgrain structure (LAB) within the lamellar α and β phases: (a) Ti-6Al-4V alloy deformed at 600℃ to 25% height reduction (LAB is depicted as red line) [9]; (b) Ti-5Al-2Sn-2Zr-4Mo-4Cr alloy deformed at 800℃ to the strain of 0.11 (LAB is depicted as yellow line) [73];(c) Ti-6Al-4V alloy deformed at 800℃ to the strain of 0.29 [74];

（3）Dynamic globularization of lamellar α

As mentioned in Section 3.3, CDRX is one of the critical mechanisms in the first stage (the formation of α/α substructure) of dynamic globularization. It could decrease the density of dislocation and then reduce the flow stress to some extent. However, many scholars have noted that the flow softening mainly occurs at low strains, when substantial dynamic globularization has not yet happen. Thus, it was concluded that the dynamic globularization of lamellar α is related to the flow softening but not a critical factor [10,32,46,59,60]. However, there is still a lack of quantitative evaluation of the effect of dynamic globularization on flow softening.

（4）Kinking of lamellar α

As described in Section 3.2, the kinking of lamellar α usually occurs at lower strains (ε<0.3), which is earlier than the dynamic globularization and corresponds to the significant flow softening. So, it was speculated that the kinking of lamellar α is one of the reasons for flow softening. And, it is explained by the reduction of bearing capacity caused by micro-buckling of lamellar α [10,32,40,41,60]. Li et al. [75] have found the positive relationship between lamellar α kinking and flow softening extent, as shown in Fig.20. However, the kinking of lamellar α is a complex process due to the local orientation and stress state dependencies. There is not yet quantitative model to estimate the role of lamellar α kinking in the flow softening of lamellar microstructure.

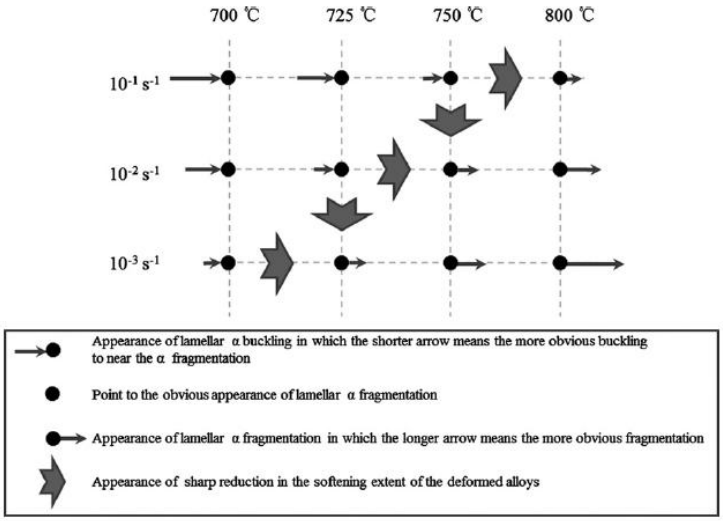

Fig.20. Schematic of the relation between α morphology characteristic and flow softening extent [75].

（5）Evolution of mechanical texture and crystallographic texture of lamellar α

It has been described in Section 3.1 that the rotation of lamellar α will make great changes of mechanical texture and crystallographic texture during deformation. The former is related to the kinking of lamellar α, while the latter greatly determines the activities of slip systems and average Taylor factor. Both of them may give rise to the flow softening of lamellar microstructure. Through the combination of polycrystalline plasticity calculations and experiment, Semiatin and Bieler [35,76] analyzed the flow behavior of a textured Ti-6Al-4V alloy with lamellar microstructure. Their calculation results suggest the crystallographic texture change lead to flow hardening rather than flow softening for all four compression directions. Hence, they concluded that the flow softening can not be explained by the crystallographic texture change per se. Even so, they got some valuable conclusions

on the flow softening behavior of lamellar microstructure: (a) the anisotropy in flow softening degree for compression of textured plate at various directions can be ascribed to the variations in texture hardening degree during deformation; (b) the flow softening degree due to microstructural effects alone can be obtained by correcting the measured flow softening degree using polycrystalline plasticity calculation.

On the other hand, Park et al. [77] connected the evolutions of crystallographic texture and mechanical texture by the following method. First, the Taylor factor of a single lamellar α was obtained according to its tilt angle from the compressive axis based on the empirical model in [39], as shown by solid line in Fig.21. Then, the average Taylor factor $\overline{M}$ at a specific strain was obtained by multiplying the fraction of lamellar α (dotted line in Fig.21) having a specific tilt angle from the compressive axis and the corresponding Taylor factor for a single α lattice (solid line in Fig.21) with a bin size of 10 and summing the values. Moreover, the variation of $\overline{M}$ with strain (Fig.22) was modeled by the following equation:

$$\overline{M} = 2.7exp\left(-\frac{\varepsilon}{0.15}\right) + 0.7log\varepsilon + 3.9 \tag{5}$$

On these bases, they evaluated the contribution of mechanical texture and crystallographic texture changes to the flow softening by:

$$\sigma = \overline{M}[\tau_0 + k_s 2^{-\frac{1}{2}}(r_0^3 + K\varepsilon/\dot{\varepsilon})^{-\frac{1}{6}}](\sigma > \sigma_p) \tag{6}$$

Where τ_0 is the friction stress, k_s is the Hall-Petch constant and r_0 is half of thickness for a non-spherical type particle at t = 0.。This equation also considers the effect of lamellar α coarsening on flow softening through Hall-Petch model (the second term in square brackets). It provided an accurate prediction of flow softening of Ti-6Al-4V alloy with lamellar microstructure during the hot compression at 815-950℃ and 0.1-1.0s^{-1}. In addition, the quantitative contribution of friction stress (related to the changes of mechanical texture and crystallographic texture of lamellar α) and Hall-Petch stress to the total stress are obtained, as shown in Fig.23.

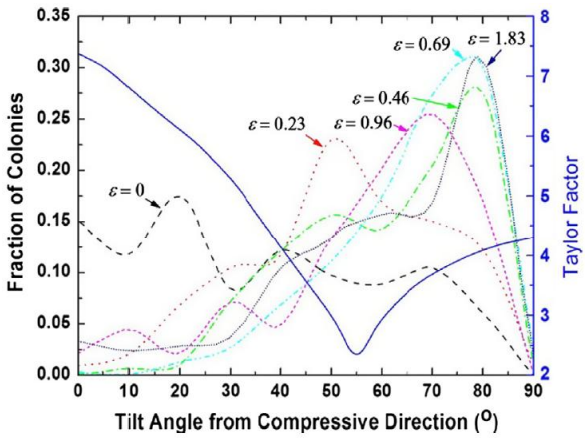

Fig.21. Fraction of lamellar α presenting different orientations with a bin size of 10º and Taylor factor for α lattice (solid line) [77].

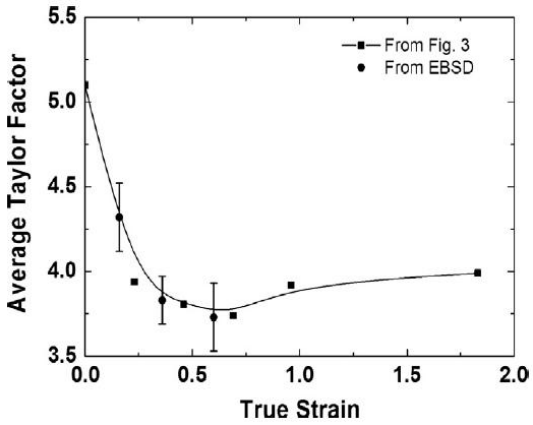

Fig.22. The variation of average Taylor factor with strain [77].

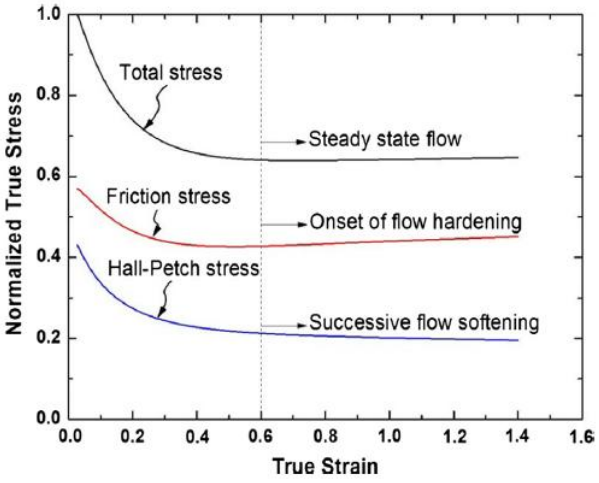

Fig.23. The contribution of friction stress and Hall-Petch stress to the total stress [77].

We can find that there are still different understandings on the effect of lamellar α rotation on flow behavior. Semiatin and Bieler [35,76] think the crystallographic texture change caused by lamellar α rotation lead to flow hardening, while, Park et al. [77] think the lamellar α rotation would lead to the

flow softening. It's difficult to determine which conclusion is right. The polycrystalline plasticity calculations in former works [35,76] mainly considers the dislocation slip and crystallographic orientation evolution of α phase. However, the effects of β phase, microstructure morphology and α/β interface on deformation behavior were not considered. For the latter work, when calculating the average Taylor factor, the c-axis of α lattice is assumed to be parallel to the trace of lamellar α. In addition, the model for variation of $\overline{M}$ with strain (eq.(6)) dose not consider the effect of initial microstructure and deformation conditions. Besides, it should be noted that the above works all focus on the role of crystallographic texture change, while the role of mechanical texture change has not got much attention. Therefore, the roles of evolutions of mechanical texture and crystallographic texture in flow behavior of lamellar microstructure still need further investigations.

（6）Loss of Hall-Petch strengthening associated with α/β interfaces

The flow softening of lamellar microstructure has also been interpreted by the loss of Hall-Petch strengthening associated with α/β interfaces [33,35]. The α/β interfaces were considered similar to the grain boundaries in single-phase materials. They acted as barriers to the dislocation movement and resulted in dislocation pileup at lower strains. With the increasing of strain, the slip transmission across α/β interfaces and concomitant loss of Hall-Petch strengthening would occur, and then lead to the flow softening. To verify the interpretation, they quantitatively compared the loss of Hall-Petch strengthening and the extent of flow softening at different deformation conditions. In order to avoid the effects of prior-beta grain size and crystallographic texture, the Ti-6Al-4V samples with various lamellar α thicknesses but almost identical prior-beta grain size and crystallographic texture were adopted in hot deformation tests. The peak stress σ_p at different conditions are measured and interpreted by the following equation:

$$\sigma_p = \overline{M}(\tau_0 + k_s l^{-\frac{1}{2}}) \tag{7}$$

where, τ_0 is the friction stress, l is the average thickness of lamellar α, and k_s is the Hall-Petch constant, which can be expressed as:

$$k_s = \left(\frac{1}{\overline{M}}\right) d\sigma_p / d(l^{-\frac{1}{2}}) \tag{8}$$

Then, taking $\overline{M}$ as 3, k_s can be determined according to the slope in the plot figure of σ_p v.s. $l^{-1/2}$. The plot figures of σ_p v.s. $l^{-1/2}$ at different conditions are shown in Fig. 24 [33]. They found that very noticeable Hall-Petch behavior exist at higher strain rates (0.1, 1, 10s^{-1}) for both 815 and 900℃. The

corresponding k_s based on σ_p v.s. $l^{-1/2}$ are given in Table 3.

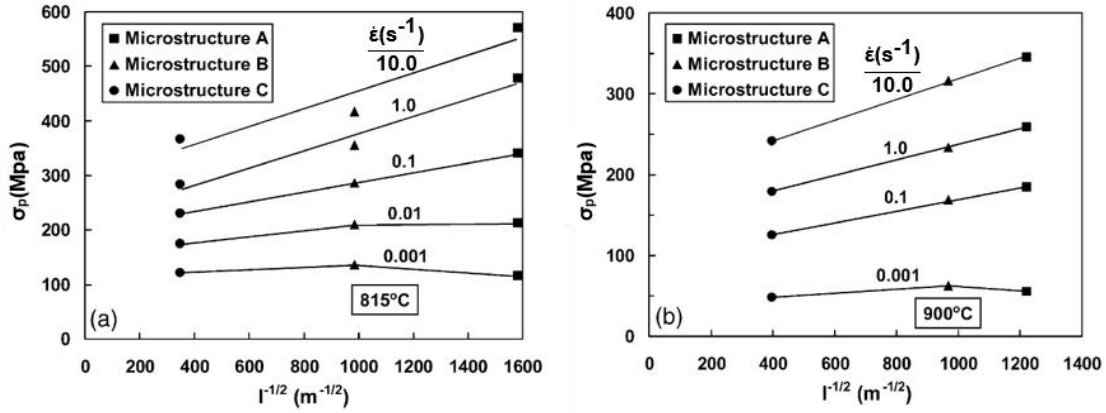

Fig.24. The peak flow stress v.s. the inverse square root of the average lamellar α thickness for Ti-6Al-4V deformed at different strain rates and temperatures of 815℃ (a) and 900℃ (b) [33].

Table 3 The Hall-Petch constants based on σ_p v.s. $l^{-1/2}$ and (σ_p-σ_{ss}) v.s. $l^{-1/2}$ at different conditions [33].

Temperature(℃)	$k_s\left(\mathrm{MPa}\sqrt{\mathrm{m}}\right)\ at\ \dot{\bar{\epsilon}}(s^{-1}) =$			$k_s{}'\left(\mathrm{MPa}\sqrt{\mathrm{m}}\right)\ at\ \dot{\epsilon}(s^{-1}) =$		
	0.1	1.0	10.0	0.1	1.0	10.0
	Based on σ_p v.s. $l^{-1/2}$			Based on (σ_p-σ_{ss}) v.s. $l^{-1/2}$		
815	0.0296	0.0526	0.0547	0.0286	0.0518	0.0537
900	0.0242	0.0322	0.0424	0.0193	0.0283	0.0442

Then, they assumed that all Hall-Petch strengthening disappear when steady state is reached, and the average Taylor factor does not change during deformation. So, the flow softening extent can be expressed by:

$$\left(\sigma_p - \sigma_{ss}\right) = M_p k_s{}' l^{-1/2} + \Delta\sigma_h \tag{9}$$

Where, M_p is approximately equal to $\overline{M}$ when all Hall–Petch strengthening disappears in the steady state. The first term at right side is the magnitude of Hall-Petch strengthening. The second term $\Delta\sigma_h$ denotes the softening increment caused by deformation heating, which is approximately constant for different lamellar α thicknesses at a given strain rate and temperature. According to eq.(10), the Hall-Petch constant ($k_s{}'$) can be determined by the slope of plot figure of (σ_p-σ_{ss}) v.s. $l^{-1/2}$, as listed in Table 3. They found that the Hall-Petch constants based on σ_p v.s. $l^{-1/2}$ and (σ_p-σ_{ss}) v.s. $l^{-1/2}$ are first-order agreement, which verifies that the loss of Hall-Petch strengthening associated with α/β interfaces is indeed an interpretation for the flow softening. Jones and Jackson [78] have observed quantities of dislocation in lamellar α (Fig.25(a)), the dislocation pileup at α/β interfaces (Fig.25(b)) and the slip transmission across α/β interfaces during the hot working of Ti-5-5-5-3 with lamellar microstructure. It provided support to the loss of Hall-Petch strengthening associated with α/β interfaces from the

physical deformation phenomenon.

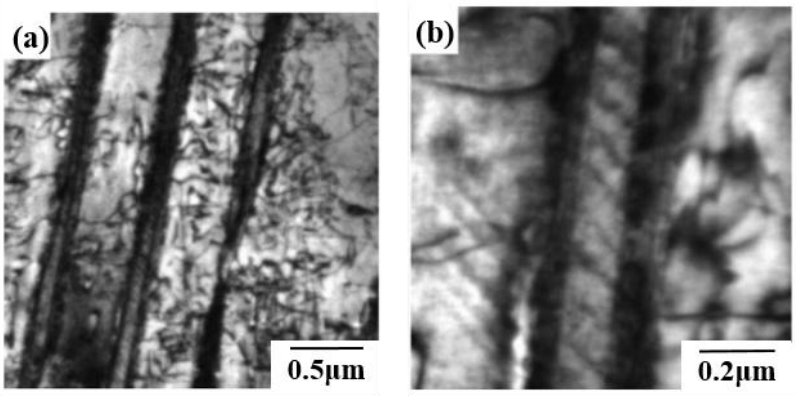

Fig.25. Bright field micrographs of Ti-5-5-5-3 deformed at 785℃ to strain of 0.1: (a) regions of high dislocation density in lamellar α, (b) slip transmission across α/β interfaces.

However, some assumptions have been made to quantitatively analyze the relationship between Hall-Petch strengthening loss and flow softening in the above works. For example, the Hall-Petch strengthening is assumed disappear totally when the steady state is reached; the average Taylor factor is assumed as a constant during deformation. Moreover, the derived contribution rates of Hall-Petch strengthening loss and deformation heating to flow softening have not been validated. Therefore, further elaborate investigations to quantify the contribution rate of Hall-Petch strengthening loss on flow softening of lamellar microstructure.

（7）Adiabatic shear band and flow localization

As well known, the adiabatic shear band and flow localization will cause the deformation resistance reduction and flow instability. Thus, it would also give rise to the flow softening to some extent. Many studies have been carried out on the formation mechanism and rules of shear band and flow localization in the hot working of titanium alloys, as mentioned in Section 3.4. However, little investigations have been conducted on the contributions of shear band and flow localization to the flow softening. It is difficult to give a quantitative evaluation on their contribution to flow softening at present.

From the above analysis, it can be concluded that the flow softening of lamellar microstructure during hot deformation is a macroscopic and synthesis outcome of many physical processes (softening mechanisms). Table 4 summarizes the reported general influence rules of deformation parameters and microstructure features on the flow softening behavior. It can be seen that the flow softening is determined by the complex interactions among many softening mechanisms operating on a wide range

of length and time scales. The effect (promotion or suppression) of a certain parameter (such as temperature or strain rate) on various softening mechanisms may be different. However, there is no informed work considered the all possible softening mechanisms thoroughly. Moreover, some conflicting assumptions were made when studying different softening mechanisms. For example, the average Taylor factor is assumed constant when studying the effect of Hall-Petch strengthening loss on flow softening [33]. While, the decrease of average Taylor factor is considered as an important factor for the flow softening when investigating the effect of mechanical texture and crystallographic texture evolutions [35,76,77]. Therefore, to elucidate the quantitative roles of each underlying physical mechanisms in flow softening, it is still needed to examine and model the internal mechanisms at a variety of scales integrally.

Table 4 Main influencing factors and laws for the flow softening of lamellar microstructure during hot deformation.

Flow softening source	Main influencing factors	General influencing laws on flow softening
Deformation heating	● Temperature ● Strain rate	Lower temperature and higher strain rate promote the deformation heating and flow softening
Evolution of dislocation substructure and dynamic recovery (DRV)		Higher temperature and lower strain rate facilitate the evolution of dislocation substructure, DRV and flow softening
Dynamic globularization of lamellar α	--	--
Kinking of lamellar α	● Temperature ● Strain rate	Lower temperature and higher strain rate promote lamellar α kinking and flow softening
Evolution of mechanical texture and crystallographic texture	● Mechanical texture and crystallographic texture of the initial microstructure ● Compression direction	--
Loss of Hall-Petch	● Temperature	Lower temperature, higher strain rate and

strengthening associated with α/β interfaces	● Strain rate ● Lamellar α thickness	smaller lamellar α thickness are beneficial to the Hall-Petch strengthening loss and flow softening
Adiabatic shear band and flow localization	● Temperature ● Strain rate	Lower temperature and higher strain rate would increase the tendency to produce adiabatic shear band, flow localization and flow softening

5. Modelling of the microstructure evolution and flow behavior

Modelling the microstructure evolution and flow behavior is of great technical significance to the microstructure tailoring and processing optimization in the TMP of titanium alloy with lamellar microstructure. At present, most studies developed the prediction models of microstructure evolution and flow behavior respectively. Only a few primary studies were conducted on the unified prediction of microstructure evolution and flow behavior considering their coupling physical mechanism. These works will be reviewed in sort in this section.

(1) Modelling of the microstructure evolution

As for the microstructure evolution, the modelling of globularization kinetic of lamellar α is the research focus. As described in Section 3.3, the experimental results show that the globularization fraction of lamellar α generally increases with strain in a sigmoid way. Thus, the Avrami-type equation (eq. (11)) has been widely employed to model the variation of globularization fraction with strain.

$$f_g = 1 - exp\,[-k \times (\varepsilon - \varepsilon_c)^n] \tag{11}$$

where, f_g is the volume fraction of globularized α, k is the kinetic constant and temperature-dependent factor, ε_c is the critical strain for initiation of dynamic globularization, n is the Avrami-exponent. In early studies, Wang et al. [57], Song et al. [58] and Ma et al. [42] have successfully applied the above equation to fit the globularization kinetics of lamellar microstructure. In these works, the parameters k, ε_c and n in Avrami-type equation were fitted based on the experimental results at some certain deformation conditions (deformation temperature and strain rate). However, the relationship between the fitted parameters and deformation conditions were not developed, so their works are not available to directly predict the globularization kinetics at any deformation condition. To overcome this problem, Song et al. [79] established the fitted parameters in Avrami-type equation with hot deformation conditions for the globularization of TC11 alloy with lamellar microstructure. The parameter k is correlated with ln$Z$ (Z is the Zener-Holloman parameter relating to temperature and strain rate) using a

liner function. The parameters ε_c and n are correlated with strain rate. Moreover, they developed the prediction model of the average grain size of globularized α (D) as the function of ln$Z$:

$$D = \begin{cases} 31.63084 - 0.61249lnZ & \dot{\varepsilon} = 0.01s^{-1} \\ 2.37124 - 0.0321lnZ & 0.1 \leq \dot{\varepsilon} \leq 10 \end{cases} \quad (12)$$

where $Z = \dot{\varepsilon}exp\left(\frac{529000}{RT}\right)$. Then they integrated the above globularization model into the FE model of cogging process of TC11 alloy, which can predict the distributions of globularization fraction and size on workpiece.

The artificial neural network (ANN) method has also been employed to model the non-linear relationship between dynamic globularization fraction and hot deformation parameters. By quantitative metallographic analysis, Wang et al. [80] obtained the dynamic globularization fraction of Ti-17 alloy under various conditions of strain, strain rate and temperature. Based on these data, they developed a back-propagation ANN model with the deformation temperature, strain and strain rate as input variables and the globularization fraction as output variables. The developed ANN model contains three layer and 12 neurons in the hidden layer. Then, they incorporated the ANN model into the macro FE model of hot compression of Ti-17 alloy, which can accurately predict the distribution of dynamic globularization fraction (Fig.26).

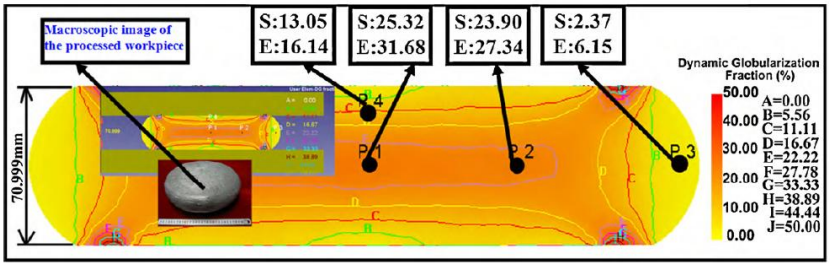

Fig.26. The comparison of globularization fraction of Ti-17 sample deformed to 45% reduction at 840℃ between experimental and predicted results by integrated model [80]. ('E' and 'S' represent experiment data and simulation results, respectively)

(2) Modelling of the flow behavior

In the recent years, FE simulation has become an important tool to optimize the hot deformation process of titanium alloy. The accurate modelling of flow behavior, i.e., the constitutive model, is one of the critical input data and greatly determines the accuracy of FE simulation. By now, the constitutive modelling for hot deformation of lamellar microstructure can be mainly classified into two types, i.e., the empirical regression model [77,81,82] and the statistical model [83,84].

The above constitutive equation (eq.(5)) proposed by Park et al. [77] is a kind of empirical regression model. As mentioned in Section 4.2, it considers the effects of rotation and coarsening of lamellar α on flow behavior. The former effect is considered by developing the regression model between the average Taylor factor $\overline{M}$ and strain. The second effect is considered by correlating the parameter *K* to deformation temperature. Their constitutive model can provided an accurate prediction of flow behavior of Ti-6Al-4V alloy with lamellar microstructure during the hot compression at 815-950℃ and 0.1-1.0s^{-1}. The classical Arrhenius-type equation (eq.(13)) has also been used to model the flow behavior of lamellar microstructure in reference [81].

$$\dot{\varepsilon} = A[\,sinh\,(\alpha\sigma)\,]^m exp\,(-\frac{Q}{RT}) \tag{13}$$

where, $\dot{\varepsilon}$ is the strain rate (s^{-1}), σ is the flow stress (MPa), *A*, *α* and *m* are the material constants for a certain strain, *Q* is the apparent activation energy for deformation, *R* is the universal gas constant and *T* is the deformation temperature. The parameters in Arrhenius-type equation were determined by regression analysis based on the experimental stresses. However, their model did not consider the effect of strain on the flow behavior, which just can predict the steady flow stress. Park et al. [82] also established an empirical regression model for the hot deformation of Ti-6Al-4V alloy with lamellar microstructures. The detailed constitutive equation is as follow:

$$\begin{cases} \sigma = \sigma^* + \sigma_u \\ \sigma^* = \left(270 + 6500C_{O,eq}\right)\left\{1 - \left[\frac{k_B T}{G_0}\left(ln\frac{\dot{\varepsilon} f(\varepsilon,T)}{\dot{\varepsilon}_0}\right)\right]^{\frac{1}{q}}\right\}^{\frac{1}{p}} \times f(\varepsilon,T) \\ f(\varepsilon,T) = 1 + a_0\left[1 - \left(\frac{T}{T_m}\right)^2\right]\varepsilon \\ \sigma_\mu = k d_{eff}^{-1/2} + \sigma_{\mu,0}^{'}\varepsilon^{n'} \end{cases} \tag{14}$$

where, σ^* is sensitive to deformation temperature and $\dot{\varepsilon}$, σ_u is insensitive to deformation temperature and $\dot{\varepsilon}$, $C_{O,eq}$ is the equivalent oxygen concentration, k_B is the Boltzmann constant, *T* is the absolute temperature, G_0 is the free energy, $f(\varepsilon,T)$ is the ratio of the initial dislocation spacing to the distance that a dislocation moves to overcome a barrier, T_m is the absolute melting temperature, and $\dot{\varepsilon}_0$ *p*, *q* and a_0 are material constants. It decomposes the flow stress into two terms, i.e., the thermally activated stress σ^* and the athermal stress σ_μ. The former stress term reflects the effects of interstitial concentration, deformation temperature and strain rate. The latter stress term reflects the effect of effective grain size of lamellar microstructure. After fitting the equation parameters, their constitutive model can well predict the flow stress at different hot deformation conditions and initial

grain sizes.

As for the statistical model, Liu et al. [83] developed a mathematical constitutive model of Ti-17 titanium alloy with lamellar microstructure based on the orthogonal analysis. Through the orthogonal experiment and variance analysis, they obtained the effect significances of deformation temperature, strain rate, strain and the interaction between temperature and strain rate to the flow behavior. Then, a multivariate nonlinear mathematical model considering the significant factors was established as follow:

$$\sigma = 0.0939(0.7277\varepsilon^2 - 1.089\varepsilon + 1.1036)[\dot{\varepsilon}\, exp\left(559.84 \times \frac{10^3}{RT}\right)]^{0.1247} \quad (15)$$

Comparison between the predicted and experimental results suggest that the above constitutive model present good prediction accuracy. Besides, Reddy et al. [84] developed a constitutive model of Ti-6Al-4V alloy with lamellar microstructure through the ANN method. The flow stress data under varying conditions of strain (0.1-0.6), strain rate (0.001-100s^{-1}) and temperature (700-1100 ℃) were obtained by continuous compression tests and applied to train the ANN model. The ANN model is a feed forward neural network including two hidden layers with a sigmoid activation function and backpropagation training algorithm. It can nicely reproduce the flow stress in sampled data and can also predict well with the non-sampled data at wide ranges of parameters. Comparing to the empirical regression model, the statistical model (especially the ANN method) present better approximation and interpolation capability and hence better prediction accuracy.

(3) Unified modelling of the microstructure evolution and flow behavior

The above separate models for the microstructure evolution and flow behavior are relatively easy to develop. However, they provide less physical insight and cannot depict the coupling effect between microstructure evolution and flow behavior. Thus, some works have been conducted to establish the physically-based internal state variable model to predict the constitutive behavior and dynamic microstructure development simultaneously in the hot deformation of titanium alloy. Babu and Lindgren [85] proposed a physically based constitutive model for Ti-6Al-4V alloy including the globularization and its effect on flow softening. This model is based on the evolution of immobile dislocation density and excess vacancy concentration. It is capable of describing the flow behavior in a wide range of temperature and strain rates by considering the dominant deformation mechanisms like dislocation pile-up, dislocation glide, thermally activated dislocation climb, globularization, etc. Bai et

al. [86] developed a set of mechanism-based unified constitutive model for the flow behavior of Ti-6Al-4V alloy, in which the dislocation density evolution, globularization of secondary lamellar α and phase transformation were considered. It can achieve the unified prediction of the flow stress and globularization of secondary lamellar α in the hot deformation. However, both of the above two models are aim to the initial bi-modal microstructure and its globularization of secondary lamellar α in β transformed matrix. They are inapplicable for the hot deformation of titanium alloy with lamellar microstructure.

Aiming at the unified prediction of flow stress and globularization evolution of lamellar microstructure, The authors proposed a set of physically based constitutive model coupling microstructure evolution [87]. In the microstructure evolution modelling, the dislocation density variation, dynamic globularization and variation of Hall-Petch strengthening were considered. The dynamic globularization modelling was realized by depicting the dependence of critical strain for globularization and globularization rate on the temperature and strain rate, as shown in eq. (16-19) [87].

$$\varepsilon_c = \varphi_0(\dot{\varepsilon}^p)^{\varphi_1}[\, exp\left(\frac{Q_{act}}{RT}\right)]^{\varphi_2} \tag{16}$$

$$\dot{X} = c_0\theta(1-X)(\dot{\varepsilon}^p)^{c_1}(\varepsilon^p - \varepsilon_c)^{c_2}M_bP/l \tag{17}$$

$$M_b = \frac{b\delta D_{ob}}{kT}exp(-\frac{Q_b}{RT}) \tag{18}$$

$$P = \rho Gb^2/2 \tag{19}$$

where, ε_c (eq.16) is the critical strain for globularization, X (eq.17) is globularization fraction, M_b (eq.18) is the grain boundary mobility, and P (eq.19) means the driving force per unit area; The detailed meaning of parameters in these equations are as follows: φ_0, φ_1 and φ_2 are material constants; θ is step function, ε^p is plastic strain, c_0, c_1, and c_2 are material constants; δ, D_{ob}, Q_b and k are the characteristic grain boundary thickness, boundary self-diffusion coefficient, boundary diffusion activation energy and Boltzmann's constant, respectively.; $Gb^2/2$ is the dislocation line energy. Then, the microstructure model was coupled into a physically based constitutive model (eq.(20)) to realize the unified prediction of flow stress and globularization evolution.

$$\sigma = \overline{M}\left\{\tau^0\left[1-\left(\frac{RT}{\Delta G}ln\frac{\dot{\varepsilon}_{ref}}{\dot{\varepsilon}^p}\right)^{1/q}\right]^{1/p} + \alpha Gb\sqrt{\rho} + K_{HP}l^{-1/2}\right\} \quad \text{where} \tag{20}$$

$\overline{M}$ is the average Taylor factor of the order of 3; τ^0 is the mechanical threshold stress, or the value of

the thermal stress at 0K, ΔG is the activation energy for deformation, R is the gas constant, $\dot{\varepsilon}_{ref}$ and $\dot{\varepsilon}^{p}$ is the reference strain rate and applied plastic strain rate, p and q are material constants. G is the shear modulus, b is the Burgers vector magnitude (2.95×10^{-10}m), ρ is the dislocation density and α is material constants; K_{HP} is the Hall-Petch coefficient, and l is the average alpha plate thickness. The material parameters in unified models were calibrated using the experimental flow stress and globularization fraction of lamellar microstructure. This model was successfully applied to simultaneously predict the flow stress and globularization evolution during hot deformation of Ti-6Al-4V and TA15 alloys at different temperatures and strain rates.

6. Conclusions

The subtransus processing is a very critical step in the whole thermomechanical processing of titanium alloy components. Its objective is to break down the lamellar microstructure after primary hot working, which plays key role in the final microstructure and performance tailoring. During subtransus processing, the microstructure evolution and deformation behavior are very complex and strongly dependent on the processing conditions and initial lamellar microstructure. Due to its great technological importance and complexity, extensive experimental and modelling investigations have been conducted on the hot working of lamellar microstructure. Many interesting progresses have been made on the laws and modelling of initial lamellar microstructure, microstructure evolution and flow behavior during this process, which provide important guidance for the optimization of subtransus processing. However, there still exist some puzzles and challenges needing more research efforts in this field as follows:

(1) Developing quantitative characterization method of globularization heterogeneity and revealing its underlying mechanisms and relation to the formation of macro-zone;

(2) Uncovering the coupling effect mechanisms of microstructure morphology, crystallographic texture, properties of α/β interface and complex strain path on the globularization heterogeneity and kinetics;

(3) Exploring and verifying the possible underlying mechanisms responsible for the significant flow softening;

(4) How to elucidate the quantitative roles of each underlying physical mechanisms in the flow softening.

(5) Developing multi-scale and multi-mechanism unified model to predict the evolutions of

microstructure morphology, crystallographic orientation and flow behavior at the same time.

(6) How to optimize the initial lamellar microstructure and processing conditions to improve the globularization kinetic and homogeneity.

Acknowledgements

The authors would like to gratefully acknowledge the support of National Natural Science Foundation of China (No. 51605388, 51875467), the Young Elite Scientists Sponsorship Program by CAST (No. 2018QNRC001), the Hong Kong Scholar Program (No. XJ2018010), the Fundamental Research Funds for the Central Universities and the Analytical & Testing Center of Northwestern Polytechnical University.

References

[1] G. Lütjering., J. C.Williams., <Titanium (2nd edition).pdf>, Springer-Verlag, Berlin Heidelberg. (2007)

[2] C. Leyens., M. Peters., <Titanium and titanium alloys.pdf>, Springer-Verlag, Berlin Heidelberg. (2003)

[3] D. Banerjee, J.C. Williams, Perspectives on Titanium Science and Technology, Acta Materialia. 61 (3) (2013) 844-879.

[4] R.R. Boyer, An overview on the use of titanium in the aerospace industry, Materials Science and Engineering A. (1996)

[5] L. Guo, X. Fan, G. Yu, H. Yang, Microstructure control techniques in primary hot working of titanium alloy bars: A review, Chinese Journal of Aeronautics. 29 (1) (2016) 30-40.

[6] S. Semiatin, V. Seetharaman, I. Weiss, The thermomechanical processing of alpha-beta titanium alloys, JOM. (1997)

[7] S. Tamirisakandala, B.V. Vedam, R.B. Bhat, Recent Advances in the Deformation Processing of Titanium Alloys, Journal of Materials Engineering and Performance. (2003)

[8] S. Semiatin, V. Seetharaman, A. Ghosh, Plastic flow, microstructure evolution, and defect formation during primary hot working of titanium and titanium aluminide alloys with lamellar colony microstructures, Philosophical Transactions of the Royal Society of London. Series A: Mathematical, Physical and Engineering Sciences. 357 (1756) (1999) 1487-1512.

[9] S. Mironov, M. Murzinova, S. Zherebtsov, G.A. Salishchev, S.L. Semiatin, Microstructure evolution during warm working of Ti–6Al–4V with a colony-α microstructure, Acta Materialia.

57 (8) (2009) 2470-2481.

[10] S. Semiatin, V. Seetharaman, I. Weiss, Flow behavior and globularization kinetics during hot working of Ti–6Al–4V with a colony alpha microstructure, Materials Science and Engineering: A. 263 (2) (1999) 257-271.

[11] J. Da Costa Teixeira, B. Appolaire, E. Aeby-Gautier, S. Denis, L. Héricher, Modeling of the phase transformations in near-β titanium alloys during the cooling after forging, Computational Materials Science. 42 (2) (2008) 266-280.

[12] J. Da Costa Teixeira, B. Appolaire, E. Aeby-Gautier, S. Denis, F. Bruneseaux, Modeling of the effect of the β phase deformation on the α phase precipitation in near-β titanium alloys, Acta Materialia. 54 (16) (2006) 4261-4271.

[13] S.M.C. van Bohemen, A. Kamp, R.H. Petrov, L.A.I. Kestens, J. Sietsma, Nucleation and variant selection of secondary α plates in a β Ti alloy, Acta Materialia. 56 (20) (2008) 5907-5914.

[14] G.C. Obasi, S. Birosca, J. Quinta da Fonseca, M. Preuss, Effect of β grain growth on variant selection and texture memory effect during α→β→α phase transformation in Ti–6 Al–4 V, Acta Materialia. 60 (3) (2012) 1048-1058.

[15] P. Gao, M. Zhan, X. Fan, Z. Lei, Y. Cai, Hot deformation behavior and microstructure evolution of TA15 titanium alloy with nonuniform microstructure, Materials Science and Engineering: A. 689 (2017) 243-251.

[16] D. Bhattacharyya, G.B. Viswanathan, R. Denkenberger, D. Furrer, H.L. Fraser, The role of crystallographic and geometrical relationships between α and β phases in an α/β titanium alloy, Acta Materialia. 51 (16) (2003) 4679-4691.

[17] D. He, J. Zhu, S. Zaefferer, D. Raabe, Effect of retained beta layer on slip transmission in Ti–6Al–2Zr–1Mo–1V near alpha titanium alloy during tensile deformation at room temperature, Materials & Design (1980-2015). 56 (2014) 937-942.

[18] D. He, J.C. Zhu, S. Zaefferer, D. Raabe, Y. Liu, Z.L. Lai, X.W. Yang, Influences of deformation strain, strain rate and cooling rate on the Burgers orientation relationship and variants morphology during β→α phase transformation in a near α titanium alloy, Materials Science and Engineering: A. 549 (2012) 20-29.

[19] D. Qiu, R. Shi, D. Zhang, W. Lu, Y. Wang, Variant selection by dislocations during α precipitation in α/β titanium alloys, Acta Materialia. 88 (2015) 218-231.

[20] S.L. Semiatin, K.T. Kinsel, A.L. Pilchak, G.A. Sargent, Effect of Process Variables on Transformation-Texture Development in Ti-6Al-4V Sheet Following Beta Heat Treatment, Metallurgical and Materials Transactions A. 44 (8) (2013) 3852-3865.

[21] S.C. Wang, M. Aindow, M.J. Starink, Effect of self-accommodation on α/α boundary populations in pure titanium, Acta Materialia. 51 (9) (2003) 2485-2503.

[22] L. Germain, N. Gey, M. Humbert, Reliability of reconstructed β-orientation maps in titanium alloys, Ultramicroscopy. 107 (12) (2007) 1129-1135.

[23] D. Qiu, P. Zhao, R. Shi, Y. Wang, W. Lu, Effect of autocatalysis on variant selection of α precipitates during phase transformation in Ti-6Al-4V alloy, Computational Materials Science. 124 (2016) 282-289.

[24] Z.B. Zhao, Q.J. Wang, Q.M. Hu, J.R. Liu, B.B. Yu, R. Yang, Effect of β (110) texture intensity on α-variant selection and microstructure morphology during β→α phase transformation in near α titanium alloy, Acta Materialia. 126 (2017) 372-382.

[25] M. Humbert, L. Germain, N. Gey, P. Bocher, M. Jahazi, Study of the variant selection in sharp textured regions of bimodal IMI 834 billet, Materials Science and Engineering: A. 430 (1-2) (2006) 157-164.

[26] M. Humbert, N. Gey, Elasticity-based model of the variant selection observed in the β to α phase transformation of a Zircalloy-4 sample, Acta Materialia. 51 (16) (2003) 4783-4790.

[27] N. Stanford, P.S. Bate, Crystallographic variant selection in Ti–6Al–4V, Acta Materialia. 52 (17) (2004) 5215-5224.

[28] N. Gey, M. Humbert, H. Moustahfid, Study of the α → β phase transformation of a Ti6Al4V sheet by means of texture change, Scripta Materialia. (2000)

[29] T. Seshacharyulu., B. Dutta., Influence of prior deformation rate on the mechanism of β→α+β transformation in Ti–6Al–4V, Scripta Materialia. (2002)

[30] S. Feng, L. Jinshan, K. Hongchao, L. Wenzhong, L. Xianghong, F. Yong, Phase Transformation during the Continuous Cooling in Near α Titanium Alloy Ti60, Rare Metal Materials and Engineering. 44 (4) (2015) 848-853.

[31] J. Xu, W. Zeng, Y. Zhao, X. Sun, Z. Du, Influence of cooling rate following heat treatment on microstructure and phase transformation for a two-phase alloy, Journal of Alloys and Compounds. 688 (2016) 301-309.

[32] E.B. Shell, S.L. Semiatin, Effect of initial microstructure on plastic flow and dynamic globularization during hot working of Ti-6Al-4V, Metallurgical and Materials Transactions A. 30 (12) (1999) 3219-3229.

[33] S.L. Semiatin, T.R. Bieler, The effect of alpha platelet thickness on plastic flow during hot working of TI–6Al–4V with a transformed microstructure, Acta Materialia. 49 (17) (2001) 3565-3573.

[34] T. Karthikeyan, A. Dasgupta, R. Khatirkar, S. Saroja, I. Samajdar, M. Vijayalakshmi, Effect of cooling rate on transformation texture and variant selection during β→α transformation in Ti–5Ta–1.8Nb alloy, Materials Science and Engineering: A. 528 (2) (2010) 549-558.

[35] S. Semiatin, T. Bieler, Effect of texture and slip mode on the anisotropy of plastic flow and flow softening during hot working of Ti-6Al-4V, Metallurgical and Materials Transactions A. 32 (7) (2001) 1787-1799.

[36] B. Perumal, M.A. Rist, S. Gungor, J.W. Brooks, M.E. Fitzpatrick, The Effect of Hot Deformation Parameters on Microstructure Evolution of the α-Phase in Ti-6Al-4V, Metallurgical and Materials Transactions A. 47 (8) (2016) 4128-4136.

[37] M. Cabibbo, S. Zherebtsov, S. Mironov, G. Salishchev, Loss of coherency and interphase α/β angular deviation from the Burgers orientation relationship in a Ti–6Al–4V alloy compressed at 800 °C, Journal of Materials Science. 48 (3) (2012) 1100-1110.

[38] S.L. Semiatin., J.F. Thomas., P. Dadras, Processing-microstructure relationships for Ti-6Al-2Sn-4Zr-2Mo-0.1Si, (1983)

[39] T.R. Bieler, S.L. Semiatin, The origins of heterogeneous deformation during primary hot working of Ti–6Al–4V, International Journal of Plasticity. 18 (9) (2002) 1165-1189.

[40] R.M. Miller, T.R. Bieler, S.L. Semiatin, Flow softening during hot working of Ti-6Al-4V with a lamellar colony microstructure, Scripta Materialia. 40 (12) (1999) 1387-1393.

[41] H. Li, Z. Zhao, H. Guo, Z. Yao, Y. Ning, X. Miao, M. Ge, Effect of initial alpha lamellar thickness on deformation behavior of a near-α high-temperature alloy during thermomechanical processing, Materials Science and Engineering: A. 682 (2017) 345-353.

[42] X. Ma, W. Zeng, F. Tian, Y. Zhou, The kinetics of dynamic globularization during hot working of a two phase titanium alloy with starting lamellar microstructure, Materials Science and Engineering: A. 548 (0) (2012) 6-11.

[43] X.G. Fan, H. Yang, S.L. Yan, P.F. Gao, J.H. Zhou, Mechanism and kinetics of static globularization in TA15 titanium alloy with transformed structure, Journal of Alloys and Compounds. 533 (2012) 1-8.

[44] N. Stefansson., S.L. Semiatin., Mechanisms of globularization of Ti-6Al-4V during static heat treatment, Metallurgical and Materials Transactions A. (2003)

[45] T. Seshacharyulu, S.C. Medeiros, J.T. Morgan, J.C. Malas, W.G. Frazier, Y.V.R.K. Prasad, Hot deformation and microstructural damage mechanisms in extra-low interstitial (ELI) grade Ti–6Al–4V, Materials Science and Engineering: A. (2000)

[46] S.A.A. Shams, S. Mirdamadi, S.M. Abbasi, D. Kim, C.S. Lee, Mechanism of Martensitic to Equiaxed Microstructure Evolution during Hot Deformation of a Near-Alpha Ti Alloy, Metallurgical and Materials Transactions A. 48 (6) (2017) 2979-2992.

[47] T. Seshacharyulu, S.C. Medeiros, J.T. Morgan, J.C. Malas, W.G. Frazier, Y.V.R.K. Prasad, Hot deformation mechanisms in ELI grade Ti-6A1-4V, (1999)

[48] M. Klimova, S. Zherebtsov, G. Salishchev, S.L. Semiatin, Influence of deformation on the Burgers orientation relationship between the α and β phases in Ti–5Al–5Mo–5V–1Cr–1Fe, Materials Science and Engineering: A. 645 (2015) 292-297.

[49] S. Roy, S. Suwas, Orientation dependent spheroidization response and macro-zone formation during sub β-transus processing of Ti-6Al-4V alloy, Acta Materialia. 134 (2017) 283-301.

[50] F. T., P. B., A.H., M. T., Dynamic recovery and recrystallization in titanium alloys by hot deformation, JOM. (2007)

[51] B. Poorganji, M. Yamaguchi, Y. Itsumi, K. Matsumoto, T. Tanaka, Y. Asa, G. Miyamoto, T. Furuhara, Microstructure evolution during deformation of a near-α titanium alloy with different initial structures in the two-phase region, Scripta Materialia. 61 (4) (2009) 419-422.

[52] J.C.M. Kampe., T.H. Courtney., Y. Leng, Shape instabilities of plate-like structures—I. Experimental observations in heavily cold worked in situ composites, (1989)

[53] L. Rayleigh, On The Instability Of Jets, Proceedings of the London Mathematical Society. (1879)

[54] S.L. Semiatin., B.C. Kirby., G.A. Salishchev., Coarsening behavior of an alpha-beta titanium alloy, Metallurgical and Materials Transactions A. (2004)

[55] L. Germain, N. Gey, M. Humbert, P. Vo, M. Jahazi, P. Bocher, Texture heterogeneities induced by subtransus processing of near α titanium alloys, Acta Materialia. 56 (16) (2008) 4298-4308.

[56] N. Gey, P. Bocher, E. Uta, L. Germain, M. Humbert, Texture and microtexture variations in a near-α titanium forged disk of bimodal microstructure, Acta Materialia. 60 (6-7) (2012) 2647-2655.

[57] K. Wang, W. Zeng, Y. Zhao, Y. Lai, Y. Zhou, Dynamic globularization kinetics during hot working of Ti-17 alloy with initial lamellar microstructure, Materials Science and Engineering: A. 527 (10–11) (2010) 2559-2566.

[58] H.-W. Song, S.-H. Zhang, M. Cheng, Dynamic globularization kinetics during hot working of a two phase titanium alloy with a colony alpha microstructure, Journal of Alloys and Compounds. 480 (2) (2009) 922-927.

[59] V. Seetharaman., S.L. Semiatin., Effect of the lamellar grain size on plastic flow behavior and microstructure evolution during hot working of a gamma titanium aluminide alloy, (2002)

[60] A.M. Zhao, H. Yang, X.G. Fan, P.F. Gao, R. Zuo, M. Meng, The flow behavior and microstructure evolution during (α + β) deformation of β wrought TA15 titanium alloy, Materials & Design. 109 (2016) 112-122.

[61] R. Poths, B. Wynne, W. Rainforth, J. Beynon, G. Angella, S. Semiatin, Effect of strain reversal on the dynamic spheroidization of Ti-6Al-4V during hot deformation, Metallurgical and Materials Transactions A. 35 (9) (2004) 2993-3001.

[62] X.G. Fan, H.J. Zheng, Y. Zhang, Z.Q. Zhang, P.F. Gao, M. Zhan, J. Liu, Acceleration of globularization during interrupted compression of a two-phase titanium alloy, Materials Science and Engineering: A. 720 (2018) 214-224.

[63] L. Li, M.Q. Li, J. Luo, Flow softening mechanism of Ti–5Al–2Sn–2Zr–4Mo–4Cr with different initial microstructures at elevated temperature deformation, Materials Science and Engineering: A. 628 (2015) 11-20.

[64] K.X. Wang, W.D. Zeng, Y.Q. Zhao, Flow behaviour and microstructural evolution of Ti‐17 alloy with lamellar microstructure during hot deformation in α+β phase field, Materials Science and Technology. 27 (1) (2011) 21-28.

[65] T. Seshacharyulu, S.C. Medeiros, W.G. Frazier, Y.V.R.K. Prasad, Microstructural mechanisms during hot working of commercial grade Ti–6Al–4V with lamellar starting structure, Materials Science and Engineering: A. 325 (1–2) (2002) 112-125.

[66] P. Wanjara, M. Jahazi, H. Monajati, S. Yue, Influence of thermomechanical processing on

microstructural evolution in near-α alloy IMI834, Materials Science and Engineering: A. 416 (1-2) (2006) 300-311.

[67] B. Wang, Z. Liu, Evaluation on fracture locus of serrated chip generation with stress triaxiality in high speed machining of Ti6Al4V, Materials & Design. 98 (2016) 68-78.

[68] C. Zheng, F. Wang, X. Cheng, J. Liu, T. Liu, Z. Zhu, K. Yang, M. Peng, D. Jin, Capturing of the propagating processes of adiabatic shear band in Ti–6Al–4V alloys under dynamic compression, Materials Science and Engineering: A. 658 (2016) 60-67.

[69] Y. Zheng, W. Zeng, Y. Wang, D. Zhou, X. Gao, High strain rate compression behavior of a heavily stabilized beta titanium alloy: Kink deformation and adiabatic shearing, Journal of Alloys and Compounds. 708 (2017) 84-92.

[70] Z.X. Zhang, S.J. Qu, A.H. Feng, J. Shen, D.L. Chen, Hot deformation behavior of Ti-6Al-4V alloy: Effect of initial microstructure, Journal of Alloys and Compounds. 718 (2017) 170-181.

[71] R.L. Goetz., S.L. Semiatin., The adiabatic correction factor and deformation heating during the uniaxial compression test, (2001)

[72] X.-p. Liang, Y. Liu, H.-z. Li, C.-x. Zhou, G.-f. Xu, Constitutive relationship for high temperature deformation of powder metallurgy Ti–47Al–2Cr–2Nb–0.2W alloy, Materials & Design. 37 (2012) 40-47.

[73] J.Z. Sun, M.Q. Li, H. Li, Initial flow softening and restoration mechanisms of isothermally compressed Ti-5Al-2Sn-2Zr-4Mo-4Cr with basketweave microstructure, Materials Science and Engineering: A. 697 (2017) 132-140.

[74] S. Zherebtsov, M. Murzinova, G. Salishchev, S.L. Semiatin, Spheroidization of the lamellar microstructure in Ti–6Al–4V alloy during warm deformation and annealing, Acta Materialia. 59 (10) (2011) 4138-4150.

[75] C. Li, X.-y. Zhang, K.-c. Zhou, C.-q. Peng, Relationship between lamellar α evolution and flow behavior during isothermal deformation of Ti–5Al–5Mo–5V–1Cr–1Fe near β titanium alloy, Materials Science and Engineering: A. 558 (2012) 668-674.

[76] S. Semiatin, T. Bieler, Effect of texture changes on flow softening during hot working of Ti-6Al-4V, Metallurgical and Materials Transactions A. 32 (7) (2001) 1871-1875.

[77] C.H. Park, J.H. Kim, Y.-T. Hyun, J.-T. Yeom, N.S. Reddy, The origins of flow softening during high-temperature deformation of a Ti–6Al–4V alloy with a lamellar microstructure, Journal of

Alloys and Compounds. 582 (0) (2014) 126-129.

[78] N.G. Jones, M. Jackson, On mechanism of flow softening in Ti–5Al–5Mo–5V–3Cr, Materials Science and Technology. 27 (6) (2013) 1025-1032.

[79] H.-w. Song, S.-h. Zhang, M. Cheng, Dynamic globularization prediction during cogging process of large size TC11 titanium alloy billet with lamellar structure, Defence Technology. (0) (2014)

[80] K.-x. Wang, W.-d. Zeng, Y.-q. Zhao, Y.-t. Shao, Y.-g. Zhou, Prediction of dynamic globularization of Ti-17 titanium alloy with initial lamellar microstructure during hot compression, Materials Science and Engineering: A. 527 (23) (2010) 6193-6199.

[81] X. Ma, W. Zeng, Y. Sun, K. Wang, Y. Lai, Y. Zhou, Modeling constitutive relationship of Ti17 titanium alloy with lamellar starting microstructure, Materials Science and Engineering: A. 538 (2012) 182-189.

[82] C.H. Park, Y.I. Son, C.S. Lee, Constitutive analysis of compressive deformation behavior of ELI-grade Ti–6Al–4V with different microstructures, Journal of Materials Science. 47 (7) (2011) 3115-3124.

[83] J. Liu, W. Zeng, Y. Lai, Z. Jia, Constitutive model of Ti17 titanium alloy with lamellar-type initial microstructure during hot deformation based on orthogonal analysis, Materials Science and Engineering: A. 597 (2014) 387-394.

[84] N.S. Reddy, C.H. Park, Y.H. Lee, C.S. Lee, Neural network modelling of flow stress in Ti–6Al–4V alloy with equiaxed and Widmanstätten microstructures, Materials Science and Technology. 24 (3) (2013) 294-301.

[85] B. Babu, L.-E. Lindgren, Dislocation density based model for plastic deformation and globularization of Ti-6Al-4V, International Journal of Plasticity. 50 (2013) 94-108.

[86] Q. Bai, J. Lin, T.A. Dean, D.S. Balint, T. Gao, Z. Zhang, Modelling of dominant softening mechanisms for Ti-6Al-4V in steady state hot forming conditions, Materials Science and Engineering: A. 559 (2013) 352-358.

[87] P. Gao, H. Yang, X. Fan, S. Zhu, Unified modeling of flow softening and globularization for hot working of two-phase titanium alloy with a lamellar colony microstructure, Journal of Alloys and Compounds. 600 (2014) 78-83.